



## TIIVISTELMÄ

Lappeenrannan teknillinen yliopisto  
LUT Energiajärjestelmät  
LUT Kone

Ivan Baulin

### **Kevytrakenteisen nestejäähdytteisen sähkökoneen rakenne – elementtien ja kokoonpanotyökalujen suunnittelu**

Diplomityö

2017

60 sivua, 39 kuvaa, 7 taulukkoa ja 4 liitettä

Tarkastaja: Professori Aki Mikkola  
TkT Scott Semken

Hakusanat: LWLC, suora nestejäähdytys, sähkökone, koneen suunnittelu, DFMA, FE-analyysi, järjestelmällinen koneensuunnittelu, ohutlevyn työstö

Tämän diplomityön tavoitteena oli keskittyä nestejäähdytteisen sähkökoneen komponenttien sekä kokoonpanoprosessin osien kehitykseen. Tutkittavat osat olivat sähkökoneen rakenteellisia komponentteja sekä kokoonpanon komponentteja. Osien kehitys toteutettiin systemaattisen koneensuunnittelun, DFMA-metodin, elementtimenetelmän, käytännön testien sekä analyttisen laskennan avulla.

Käytännön testit osoittivat, että voidellulla lasikuitupultilla toteutettu ruuviliitos tuottaa 48 % korkeamman puristusvoiman kuin kuivalla pulttiliitoksella. Muuntajateräslaminaattien pinnoitetestin tuloksien perusteella SURALAC 7000 -pinnoite valittiin sopivaksi pinnoitteeksi. Roottorin ja staattorin kiekkokokoonpanojen puristuskiinnikkeiden materiaalipaksuus määritettiin FE-analyysin sekä käsilaskujen avulla. Tulosten perusteella 0,5 mm ruostumaton jousiteräs valittiin sopivaksi materiaaliksi. Balsa-puu osien koneistusmenetelmäksi valittiin CNC-jyrsintä sen osoittauduttua sopivaksi kahden työstetyn näytekappaleen perusteella. Kiekkokokoonpanojen kokoamista varten rakennettiin asennuspöytä. Kokoamisprosessin helpottamiseksi kehitettiin työkalut, jotka asennettiin asennuspöydän ja kiekkokokoonpanon väliin.

## **ABSTRACT**

Lappeenranta University of Technology  
LUT School of Energy Systems  
LUT Mechanical Engineering

Ivan Baulin

### **Design of Structural Elements and Assembly Tools for LWLC Electrical Drive**

Master's thesis

2017

60 pages, 39 figures, 7 tables and 4 appendices

Examiner: Professor Aki Mikkola  
D. Sc. (Tech.) Scott Semken

Keywords: LWLC, direct liquid cooling, electrical drive, machine design, DFMA, FE analysis, systematic engineering, sheet metalworking

The goal of this master's thesis was concentrated on development of detail parts for LWLC electrical machine and its assembly. The parts that were studied in this thesis were structural elements of wheel face of the machine and its segments. Tools for the assembly of LWLC machine were also studied. The development of parts was done using systematic engineering design, DFMA method, FE method, practical tests and analytical calculation.

The results of practical tests showed that lubricated fiberglass stud bolt joint can provide 48 % higher binding force compared to non-lubricated joint. The test of coatings for electrical steel laminations showed that SURALAC 7000 was acceptable coating. The material thickness of wheel face lamination clamps was determined through FE analysis and analytical calculations. As a result 0,5 mm thick stainless spring steel was chosen as a material for wheel face lamination clamps. CNC milling was considered as the most appropriate manufacturing process for balsa wood spacers after two test pieces were cut by CNC milling machine. A torsion box was built for realizing assembly of wheel face. Wheel face assembly spacers were developed in order to assist in the assembly process of the wheel face.

## ACKNOWLEDGEMENTS

I would like to express my gratitude to Professor Aki Mikkola and D. Sc. (Tech.) Scott Semken for the opportunity to work with this project and write my thesis at LUT. Thank you Aki for supervising my thesis and giving feedback during the writing process. Thank you Scott for guiding through the design process and during practical tests.

I want to thank my mother and my relatives for the support I had during my studies in Lappeenranta and during the time I was writing this thesis. Without the support I had it would have been much more difficult to manage through these six years.

I can't imagine my years at the university without all the friends I made here. Thank you all for making these six years a unique time. A big thanks to Koneenrakennuskilta and its active members for all the events and trips I was able to participate in. Being a member of the board of Koneenrakennuskilta gave me opportunities to meet many great persons from other student guilds as well, and I am grateful for that.

I would also like to thank mentors at ESN BME and all the people I met during my exchange time in Budapest for a great spring semester of 2016.

“Because in a split second, it's gone.” – Ayrton Senna

*Ivan Baulin*

Ivan Baulin

Lappeenranta 8.5.2017

## CONTENTS

### TIIVISTELMÄ

### ABSTRACT

### ACKNOWLEDGEMENTS

### CONTENTS

### LIST OF SYMBOLS AND ABBREVIATIONS

|          |   |    |
|----------|---|----|
| <b>1</b> | <b>INTRODUCTION</b> .....                           | 8  |
| 1.1      | Background .....                                    | 8  |
| 1.2      | Objectives and Scope .....                          | 10 |
| 1.2.1    | Challenge .....                                     | 11 |
| <b>2</b> | <b>LWLC STRUCTURAL ELEMENT DEVELOPMENT</b> .....    | 12 |
| 2.1      | The Systematic Approach to Engineering Design ..... | 12 |
| 2.1.1    | Solution finding methods .....                      | 13 |
| 2.2      | General Problem Solving Process .....               | 13 |
| 2.3      | Requirements List and Classification Scheme .....   | 15 |
| 2.4      | Finite Element Method .....                         | 16 |
| 2.5      | Design for Manufacture and Assembly .....           | 17 |
| 2.5.1    | Advantages of DFMA .....                            | 19 |
| 2.5.2    | Cases when DFMA may not be used .....               | 19 |
| 2.6      | Sheet Metalworking .....                            | 20 |
| 2.6.1    | Forming Operations .....                            | 21 |
| 2.6.2    | Cutting Operations .....                            | 23 |
| <b>3</b> | <b>RESEARCH RESULTS</b> .....                       | 27 |
| 3.1      | Binding rods for rotor and stator segments .....    | 27 |
| 3.1.1    | Binding Force .....                                 | 28 |
| 3.2      | Wheel face lamination clamps .....                  | 32 |
| 3.2.1    | Clamping force .....                                | 32 |
| 3.3      | Balsa wood spacers .....                            | 39 |
| 3.4      | Non-oriented Electrical Steel Laminations .....     | 41 |
| 3.4.1    | Coatings .....                                      | 42 |
| 3.5      | Torsion Box .....                                   | 45 |

3.5.1 Wheel Face Assembly Spacer Tools .....47

4 **CONCLUSIONS** .....52

**REFERENCES**.....57

**APPENDICES**

Appendix I: Clamping force calculations

Appendix II: Result charts of fiberglass vinyl ester stud bolt test

## LIST OF SYMBOLS AND ABBREVIATIONS

|                |   |
|----------------|---|
| $A_{rod}$      | Effective cross-section area of fiberglass vinyl ester stud bolt [mm <sup>2</sup> ] |
| $E_c$          | Elastic modulus of clamp material [MPa]   |
| $F_{bind}$     | Binding force of fiberglass vinyl ester stud bolt [N]                               |
| $F_c$          | Clamping load [N]   |
| $I_c$          | Moment of inertia of the simplified clamp [mm <sup>4</sup> ]                        |
| $a_c$          | Distance of clamping load from fixed end [mm]                                       |
| $f_c$          | Displacement of the free end of the simplified clamp [mm]                           |
| $k_{spr}$      | Spring constant of ST53250 Raymond Die spring [N/mm]                                |
| $l_c$          | Total length of the simplified clamp [mm]   |
| $x_{spr}$      | Displacement of ST53250 Raymond Die spring [mm]                                     |
| $\sigma_{rod}$ | Tension in fiberglass vinyl ester stud bolt [MPa]                                   |
| CAD            | Computer Aided Design   |
| CNC            | Computer Numerically Controlled   |
| DFA            | Design for Assembly   |
| DFM            | Design for Manufacture  |
| DFMA           | Design for Manufacture and Assembly   |
| DLC            | Direct Liquid Cooled  |
| EES            | European Electrical Steels  |
| FE             | Finite Element  |
| LWLC           | Lightweight Liquid Cooled   |
| Nd: YAG        | Neodymium Yttrium – Aluminum – Garnet   |
| OD             | Outer diameter  |
| PMSG           | Permanent Magnet Synchronous Generator  |
| PMSM           | Permanent Magnet Synchronous Motor  |

## 1 INTRODUCTION

Industrial applications require high efficiency and accurate dynamic performance, which increases the need for new types of motors. Compared to induction motors efficiency and power factor of PMSM (Permanent magnet synchronous motor) does not depend on the number of pole pairs and speed in the same way. Therefore PMSM can be used in new adjustable speed AC (Alternating current) inverter drives. Use of direct drive PMSM enables the replacement of induction motor and mechanical gearbox. Replacement of induction motor and gearbox combination with direct drive PMSM can provide savings in space, increased efficiency and lower maintenance costs. (Heikkilä 2002, p. 1.)

The direct driven machine can be used in wind power plants as the replacement for generator-gearbox combination. Gearless wind turbines can reduce disadvantages such as noise, weight, maintenance demands and maintenance difficulties. (Lampola 2000, p. 9.)

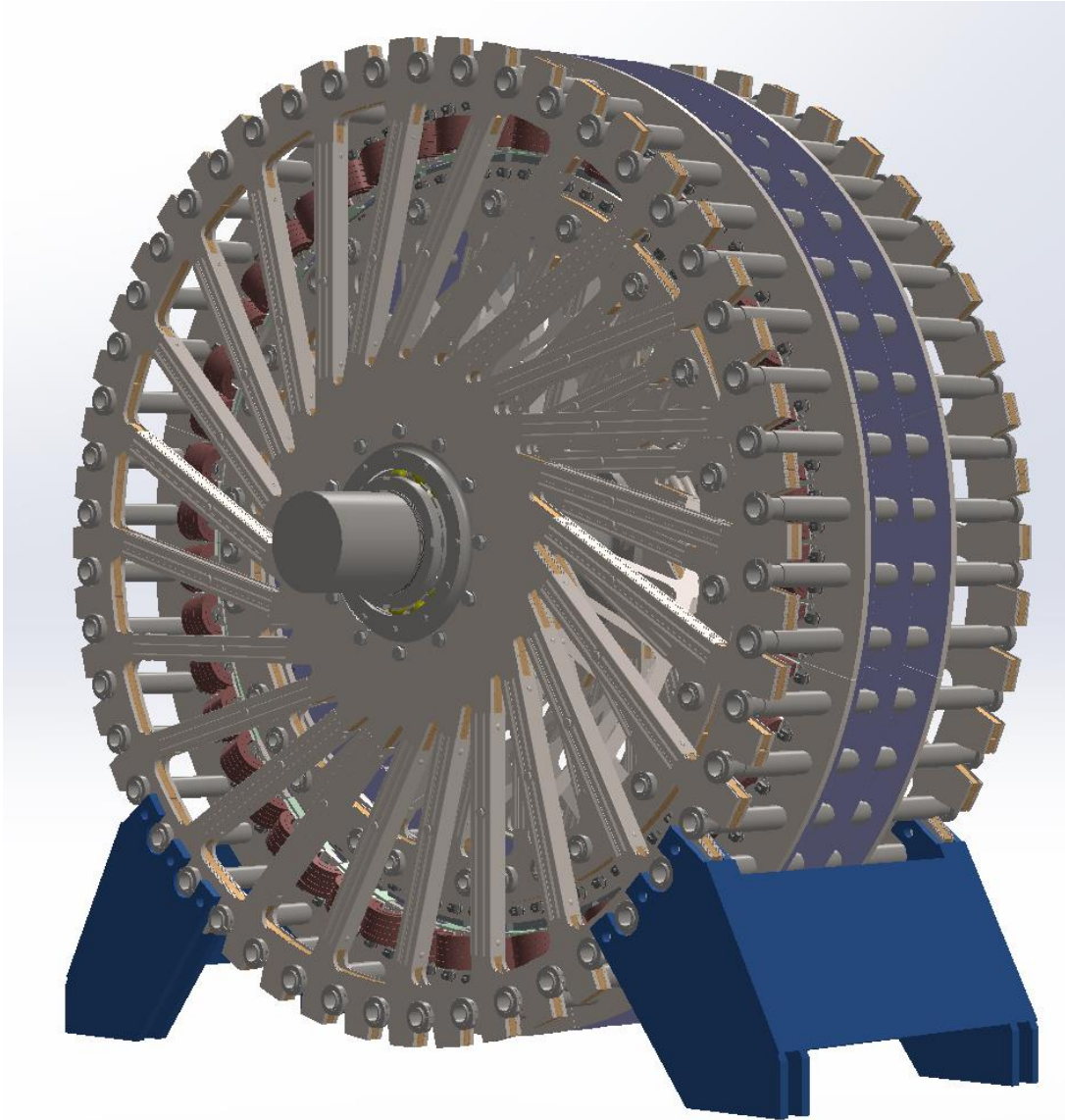
### 1.1 Background

Most of the operational wind turbines are land based. The number of offshore wind turbines has been increasing among new installations mainly because higher amount of wind at the offshore sites. In order to respond to demands of offshore wind turbines the reliability of turbines has to be good. This means frequent maintenance of the turbine and duration of the maintenance process have to be reduced. The need of improved reliability contributes to development of direct-driven generator solutions. (Semken 2015, p. 46.)

Direct-drive solutions, especially low-speed, high-torque generators enable the operation of wind turbines without complex gearbox configurations. Heavy gearbox solutions used in medium- or high-speed generators are important source of turbine failures. This means direct-drive generators can reduce maintenance of wind turbines, improve reliability and for example direct-drive PMSG (Permanent Magnet Synchronized Generator) can provide good overall efficiency. (Semken 2015, p. 46.)

A new lightweight architecture for PMSG with less massive structures of stator and rotor that has been developed at LUT (Lappeenranta University of Technology) can be seen in

figure 1. The new structure of PMSG which is based on DLC (Direct Liquid Cooled) tooth-coil windings can provide excellent properties for example for wind power industry. Lightweight structure of LUT team's machine can be reliable and cost effective. (Semken 2015, p. 30.)



**Figure 1.** Lightweight generator structure developed at LUT.

In order to increase power capacity of direct-drive PMSG the power density must be increased. The increase of power density can be accomplished by increasing linear current density in stator coils, which results in increased heat generation. The material for winding conductor in thermally insulated stator windings is copper, which has high thermal conductivity. The heat flows freely along the conductor. However out of the conductor and through the insulation heat flow is significantly reduced, which leads to direct cooling of the

copper conductor being the best cooling solution. The DLC tooth-coil windings enable effective heat-removal from direct-drive PMSG as liquid coolant is flowing inside the copper conductor. (Semken et al. 2012, p. 6-7.)

The proposed PMSG structure is based on slanted-spoke design of the wheels of stator and rotor, as can be seen from figure 1. The design is used to control the deformation of the wheels and maintain air gap between rotor and stator without excess steel material (Semken 2015, p. 101). The slanted-spoke design of LUT's machine is built by using sheet-steel layers that can provide structural integrity and remarkably higher structural damping in perpendicular direction to the stack when appropriately bound. Another element that is used to increase damping in axial direction is spacers between wheel faces. The structural integrity is achieved from friction between sheet-steel elements, which means the wheels can be built without welding. By eliminating welds the fatigue crack propagation and failures in welded connections can be eliminated and manufacturing costs can be reduced. (Nutakor et al. 2015)

## 1.2 Objectives and Scope

The objective of this work is to determine suitable detail components for LWLC (Lightweight Liquid Cooled) electrical drive and its assembly. The research will concentrate on a number of details of the LWLC machine, such as binding rods for rotor and stator segment laminations, wheel face laminations' clamping, balsa wood spacers and wheel face assembly tools. Binding rods and wheel face laminations' clamps will be examined from the perspective of forces in order to establish binding force and clamping force required for the machine. The examination of balsa wood spacers will be focused on material properties of balsa wood and the purpose of spacer parts in LWLC machine. The assembly tools will be examined from the perspective of assembly of wheel faces.

The research process will include 3D drawing of some parts by using CAD (Computer Aided Design) software, which will be also used to provide technical documentation. FE (Finite Element) analysis software will be used during the research if necessary. In order to produce parts that are manufacturable and easy to assemble, DFMA (Design for Manufacturing and Assembly) perspective will be taken into account. Some analytical calculations and practical experiments will be used to confirm reliability of certain parts of the assembly. Prototype

parts will be made in collaboration with university laboratories or subcontractors, depending on the manufacturability of the parts. Necessary changes in part design will be made in order to establish functional design of individual parts. The results and data from this work will be used in building a full-scale working prototypes of the LWLC electrical drive.

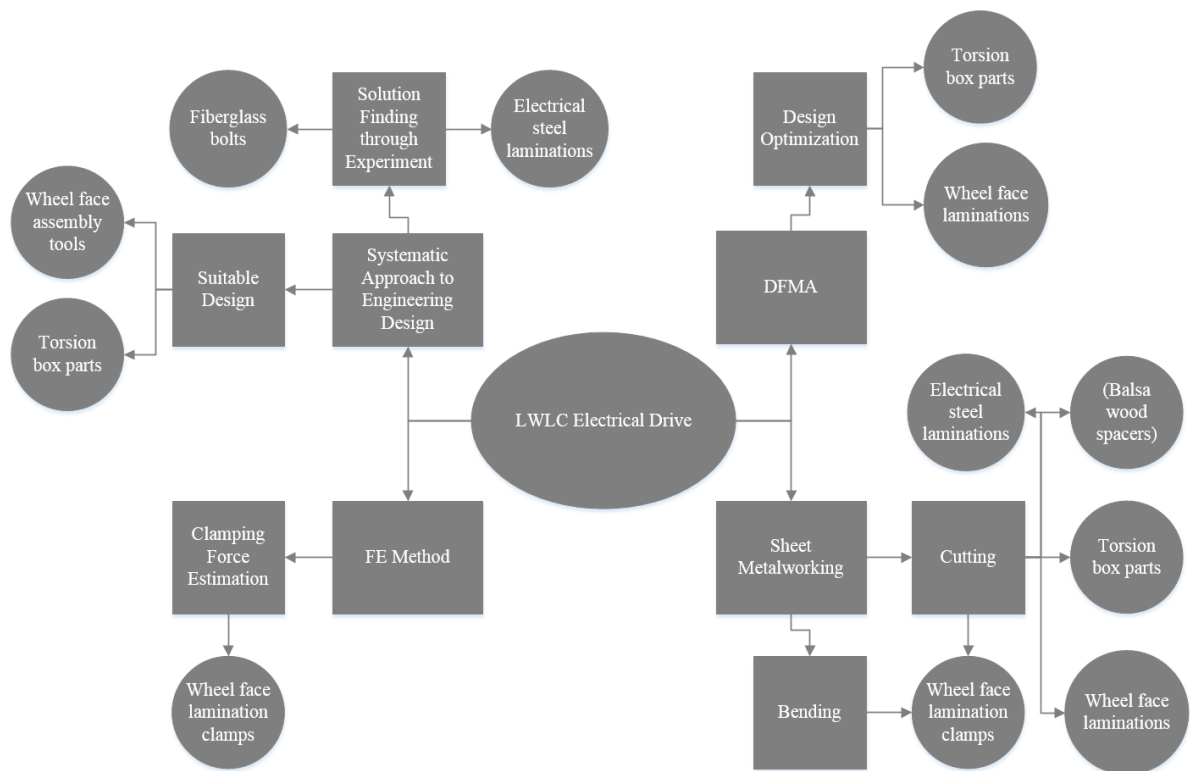
### 1.2.1 Challenge

Selecting suitable components for LWLC machine can be seen as a challenge in this work. Some of the detailed parts of LWLC machine will have to be designed, manufactured and tested in order to establish their compatibility. First challenge in design may be little amount of information regarding the parts, which means in some cases initial information must be estimated. Second challenge in design may be manufacturability of the parts and finding a subcontractor that can manufacture the parts. This challenge might be important in cases when uncommon materials will be used. Third challenge may occur while testing the parts. If designed and manufactured parts will not fit the machine, they will have to be redesigned. There is also a chance of rapid changes in the design of the machine, which may also lead to re-design process.

Some of the materials used in the structure of the LWLC machine may not be common for manufacturers in Finland, which can also be seen as a challenge. In case if Finnish companies, metal workshops or merchants will not be able to provide required material, finding and buying the material might prove challenging.

## 2 LWLC STRUCTURAL ELEMENT DEVELOPMENT

In this chapter theories of systematic approach of engineering design, FE method and DFMA are presented. The systematic approach is presented from the perspective of solution finding, general problem solving and solution classification. FE method is presented briefly, including basic theory. DFMA is approached from the advantages' point of view and also not using of DFMA is discussed. Figure 2 shows how each method is exploited in this thesis.



**Figure 2.** Used methods and their areas of exploitation.

Basic information about working with sheet metal is also presented in this chapter as can be seen from figure 2, with information about bending sheet metal with press brake and cutting sheet metal with laser cutting and punching.

### 2.1 The Systematic Approach to Engineering Design

The systematic approach can be used by designers in finding optimal solution. It gives more flexibility to designers when they try to develop suitable ideas, because relevant methods can be used when solutions are systematically elaborated. In order to find optimal solution

for given task a range of potential solutions has to be generated with function structure, in which overall task is divided into subtasks. To realize each of subtasks a number of possible physical effects is set according to task-specific requirements. The solution finding methods are good to be used as subfunctions may only be realized with combinations of physical effects. Depending on the problem, different type of solution finding method can be used. (Pahl et al. 2007, p. 77-78.)

### 2.1.1 Solution finding methods

Information gathering can be seen as an important method for designers to gain access to high quality information. Common techniques of information gathering such as literature searching, patent exploring and trade publication analyzing can be effectively exploited by the internet. (Pahl et al. 2007, p. 78-79.)

The existing technical systems can be analyzed in order to find solutions. Especially when new solutions are created or old ones are improved the analysis of technical systems is important method. Finished products are divided into pieces mentally or physically during the process, in which the goal is to discover related physical, embodiment and logical design features. Possible systems that are used for analysis are:

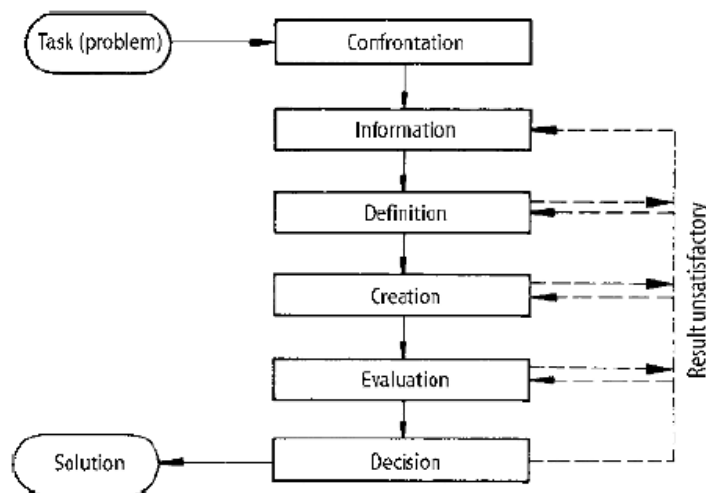
- product ideas or production methods of competitors
- own company's out-of-date products and production methods
- similar subfunctions of products or assemblies to those solutions that are sought.

In other words this method can be called the systematic exploitation of existing products or experience. As a result designers may hold on to old solutions instead of finding new ones, which can be seen as a risk. A vital information can also be obtained from experimental studies, model tests and measurements. These empirically based sources of information are important in mass production industries and precision engineering. (Pahl et al. 2007, p. 81-82.)

## 2.2 General Problem Solving Process

To find a satisfactory solution iteration method can be used, in which a solution is approached step-by-step. The iteration loop is used mainly because of complex

interrelationships between individual steps and information requirements at each step. This means information required in one step may be provided by a subsequent step. The aim of systematic approach is making design work effective and efficient by keeping iteration loops small. (Pahl et al. 2007, p. 126.) The chart of general problem solving process is shown in figure 3.

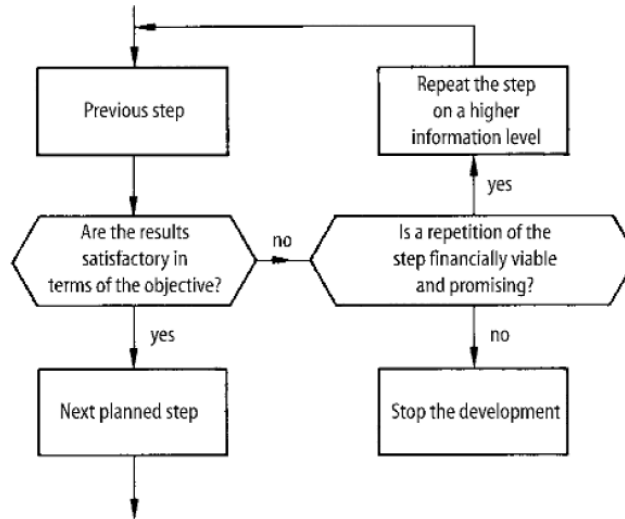


**Figure 3.** Steps of general problem solving process (Pahl et al. 2007, p. 127).

As seen from figure 3 first step of the problem solving process is confrontation. The initial step involves clarifying of the problem and determining known and unknown information. Previous knowledge in the field of the given task can be seen as advantage of a designer as the knowledge can be used effectively in clarifying requirements and their types. (Pahl et al. 2007, p. 126.)

After the problem is confronted and necessary information is gathered, the essential problems are defined in definition phase. The definition is done on abstract level to set main constraints, which enables unconstrained search for solutions and searching for unconventional solutions. The last three steps of general problem solving process are used to create, evaluate and decide the solution in order to achieve the overall objective. During the creation phase different methods are used to create a number of solutions that are evaluated in case if the number of proposed solutions is high. The best solutions are selected during decision phase. (Pahl et al. 2007, p. 126-127.)

During the decision phase general decision making process is used. The process consists of six steps in total as shown in figure 4.



**Figure 4.** Steps of general decision making process (Pahl et al. 2007, p. 127).

As figure 4 illustrates the decision making process can be done in three steps, depending on the nature of achieved results. If results from earlier step are satisfactory, the process can be carried on to the next step. In case if results do not meet the goal the next step cannot be taken and previous step may be repeated from more detailed perspective within the limits of available resources. If there are no available resources to repeat the previous step, the development of the idea should be stopped or the objective should be entirely or partially changed, as the results may be valuable for other applications. (Pahl et al. 2007, p. 128.)

### 2.3 Requirements List and Classification Scheme

In order to set up the requirements for a product the basic data has to be collected. Setting up the requirements can be divided in two steps: definition of obvious requirements and extension of these requirements. Definition of goals and circumstances which given goals have to meet has to be clearly made. The results can be classified as demands and wishes. Demands must be fulfilled under all circumstances in order for solution to be acceptable. Wishes are requirement type that should be taken into account if possible, but they don't affect the decision whether the solution is acceptable or not. Wishes can be grouped according to their importance in three groups: major, medium or minor. The least information that should be included in the requirement list consists of user, project or product

name, requirement labels, responsible person, date of issue and the last change, version number and page number. (Pahl et al. 2007, p. 146-147.)

A classification scheme can be used when several subfunctions require solutions. In this case the functions can be selected as classifying criteria. In the scheme subfunctions are presented in columns and solutions are presented in rows as shown in figure 5. (Pahl et al. 2007, p. 182.)

| Sub-functions | Solutions | 1        | 2        | ...      | $j$      | ...      | $m$      |
|---------------|-----------|----------|----------|----------|----------|----------|----------|
|               | 1         | $F_1$    | $S_{11}$ | $S_{12}$ |          | $S_{1j}$ |          |
| 2             | $F_2$     | $S_{21}$ | $S_{22}$ |          | $S_{2j}$ |          | $S_{2m}$ |
| $\vdots$      | $\vdots$  | $\vdots$ | $\vdots$ |          | $\vdots$ |          | $\vdots$ |
| $i$           | $F_i$     | $S_{i1}$ | $S_{i2}$ |          | $S_{ij}$ |          | $S_{im}$ |
| $\vdots$      | $\vdots$  | $\vdots$ | $\vdots$ |          | $\vdots$ |          | $\vdots$ |
| $n$           | $F_n$     | $S_{n1}$ | $S_{n2}$ |          | $S_{nj}$ |          | $S_{nm}$ |

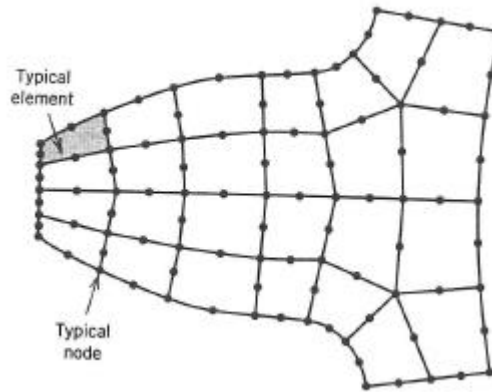
**Figure 5.** Structure of classification scheme (Pahl et al. 2007, p. 182).

Classification scheme shown in figure 5 is useful in systematic combination, in which different solutions for each subfunction can be combined. During the combination at least one solution for each subfunction must be used. The challenge in systematic combination is to find compatible solutions, which means theoretically possible solutions have to be narrowed to practically possible solutions. (Pahl et al. 2007, p. 104.)

#### 2.4 Finite Element Method

FE method is used to solve specific problems, for example stress field in stress analysis, numerically and typically users are interested in peak values of field quantity or its gradients. Results for simple problems can be treated as accurate results, but for complicated problems results are approximate. FE method can be simply described as procedure in which a structure is divided into number of elements. Behavior of each element is described and elements are connected together at nodes. Principle of mesh used in FE method is shown in figure 6. As a result there are algebraic equations which in stress analysis are equilibrium

equations of the nodes. The number of equations may be hundreds or thousands, which requires use of computer. (Cook 1995, p. 1.)

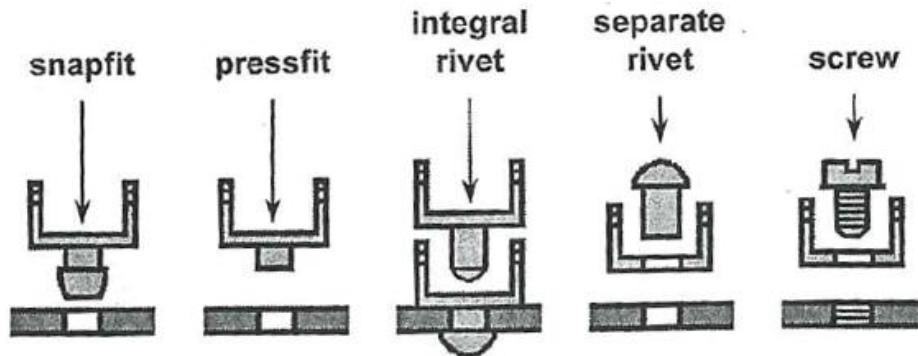


**Figure 6.** Elements and nodes in a meshed structure (Cook 1995, p.2).

Commercial software is used to solve problems with FE method, because the FE theory consists of matrix manipulations, solving of equations, numerical integration and other procedures that are solved automatically by computer. As a result the user does not see the whole procedure, but some parts of it when data is processed. The most important steps from perspective of the user are preprocessing and postprocessing. During preprocessing step loads, constraints, material properties and mesh are defined by the user. Postprocessing is used for output sorting, listing and plotting of results of an analysis. The accurate work done during preprocessing and postprocessing may aid the user, but it does not affect the accuracy of the achieved results of FE analysis. (Cook 1995, p. 2.)

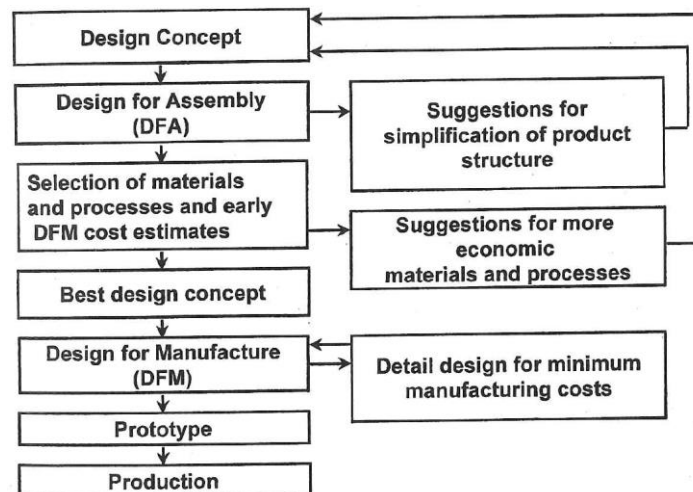
## 2.5 Design for Manufacture and Assembly

The term DFMA results from combination of terms DFM (Design for Manufacture) and DFA (Design for Assembly). DFMA method is used to aid designers to produce simplified products in order to reduce manufacturing and assembly costs, to quantify difficulties in assembly and manufacturing by studying competing products and to negotiate contracts with suppliers. During the development stages of DFM and DFA in 1960's and 1970's the goal was to reduce the number of parts in assembly and to design easily manufacturable products. Figure 7 illustrates how more simple designs may affect the assembly. (Boothroyd, Dewhurst, Knight 2002, p. 1-2.)



**Figure 7.** Designs that affect the assembly (Boothroyd et al. 2002, p. 2).

The ability of estimating manufacturing and assembly costs during the early stage of design process can be seen as the essence of DFMA, because over 70 % of final product costs are defined during a product design process. Consideration of DFA and DFM during the early stages of design can reduce assembly and manufacture costs of a product and help in developing a prototype which would be put into production. Figure 8 shows the function of DFA and DFM inside the DFMA process. (Boothroyd et al. 2002, p. 4-5.)

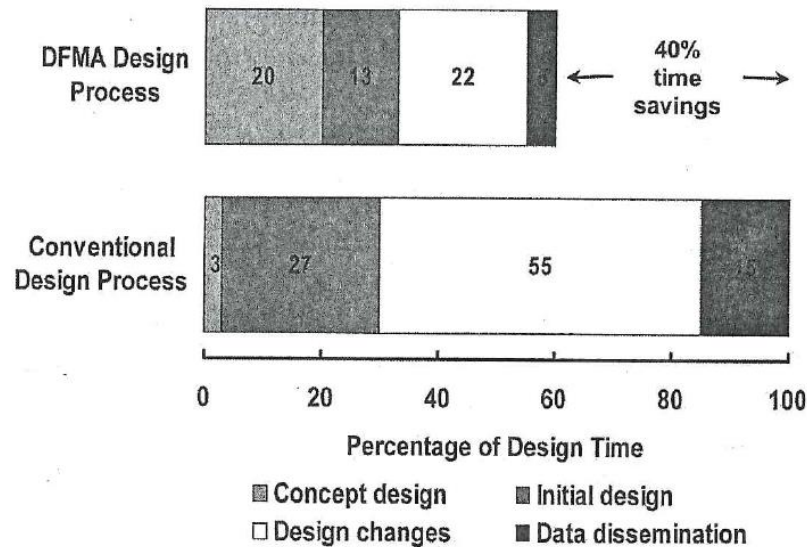


**Figure 8.** Steps used in DFMA method (Boothroyd et al. 2002, p. 15).

As can be seen from figure 8 the DFA perspective can provide help in determining possible simplifications of a product. Early cost estimates for DFM are used for both original design and updated design to compare trade-offs between the designs. A more specific DFM analysis is made after the final selection of materials and processes is found. (Boothroyd et al. 2002, p. 15.)

### 2.5.1 Advantages of DFMA

In addition to reduced assembly times and manufacturing costs DFMA affects the quality and reliability, manufacturing cycle time and time to market. Figure 9 shows the comparison between DFMA design and conventional design processes.



**Figure 9.** Using DFMA design process time spent can be reduced by 40% (Boothroyd et al. 2002, p. 6).

Also the systematic approach to analyzing a design from perspective of manufacture and assembly can be seen as an advantage of DFMA. The systematic approach provides simpler products with higher reliability at lower costs. By exploiting the DFMA process the teamwork is encouraged between designers and manufacturers. This leads to the situation where traditional “over-the-wall approach” can be avoided and therefore conflicts between design and manufacture can be solved. (Boothroyd et al. 2002, p. 7, 21-22.)

### 2.5.2 Cases when DFMA may not be used

DFMA has its advantages as mentioned earlier but there can be some cases observed when DFMA may not be implemented. The most common case is restricted time for designers to come up with a design of a product. Executives and managers of companies may not see the effect of the early stages of design process on overall DFM cycle time, as they constrain designers with work time in order to minimize DFM time. Another case including executives and managers is applying DFMA. Usually executives or managers are the first to hear of

benefits of DFMA which results in demand of DMFA implementation. Designers may not support the idea if they are not involved in decision process or it is not their proposal to use DFMA. (Boothroyd et al. 2002, p. 16.)

As mentioned in paragraph 2.5 the first step in DFMA process is DFA analysis. For a particular part or product assembly costs may form small part of total manufacturing costs, which might lead to DFA analysis not being used. Therefore DFMA process may be considered unnecessary. Also the volume of a product may affect the implementation of DFMA. Common expression is that DFMA is worth using only for high-volume products. DFMA may be not used for low-volume products because original design of a product may not be reconsidered, which results in thought of making right design on first try being superior. In some cases designer's own philosophy may be the key factor for implementing DFMA or not. If a designer doesn't like the process or company has used some other methods in the past, the implementation of DFMA may not work. (Boothroyd et al. 2002, p. 16-21.)

## 2.6 Sheet Metalworking

There are two fundamentally different ways to manufacture parts from sheet metal. The first method involves using of individually made dies to shear pieces of required shape from the steel strip. The strip may be in specific length, cut from metal sheets, or in coil form. In the shearing process the metal sheet is fed automatically from the coil or manually loaded into vertical press on which the die is mounted. Dies may also be used to change the shape of the blanks using stretching, compressing or bending. Also by using dies in piercing operations additional features may be added. (Boothroyd et al. 2002, p. 381.)

In the second method CNC (Computer Numerically Controlled) punching machines are used to make sheet metal parts from individual sheets in large quantities. CNC punching machines are capable of doing various punches because of rotating turrets, in which different tools can be stored. During the punching operation the machine first produces all the internal features of a part, after which the external lines are punched or profile cut. Profile cutting can be done by laser or plasma cutter that can be mounted to the press machine. (Boothroyd et al. 2002, p. 381.)

Conventional metal cutting methods can also be used on stainless steel but higher forces are required as stainless steel has higher yield strength than carbon steels. For performing cutting operations for stainless steel it is preferable to have stainless steel in annealed form. Common ways to cut stainless steel are: laser cutting, water jet cutting and plasma cutting. When cutting stainless steel there is a risk of oxidation of the surface and therefore corrosion resistance of the material may be weakened. Because of the risk of oxidation of the surface, an inert gas such as nitrogen is used when cutting stainless steel. Cutting with the assist of inert gas may leave burr on the bottom surface of the workpiece if cutting parameters are incorrect. (Matilainen et al. 2011, p. 50, 159.)

### 2.6.1 Forming Operations

The most used forming operation for sheet metal is bending with press brake. During the bending operation strains and stresses are formed in the metal sheet. According to formed strains and stresses bending can be divided in three phases:

- elastic bending
- elastic – plastic bending
- plastic bending.

In elastic bending the sheet returns to its initial form after bending force is removed, because the yield strength of the material is not exceeded. During the elastic – plastic bending some areas of the sheet exceed yield strength. As a result after removing bending force some areas of the sheet return to initial form and some areas stay in bended form. In plastic bending phase the number of elastic areas in the sheet is small and the bending can be considered as plastic. (Matilainen et al. 2011, p. 239.)

Press brakes used for bending sheet metal are typically 2–4 meters wide but the width can vary between 1 and 10 meters. An example of press brake machine is shown in figure 10. The longest possible bending length can be determined from nominal width of the machine and machines can be linked together in series in order to bend long workpieces. The bending force depends on the material and thickness of the sheet but it can vary in 100–25000 kN range. (Matilainen et al. 2011, p. 240.)



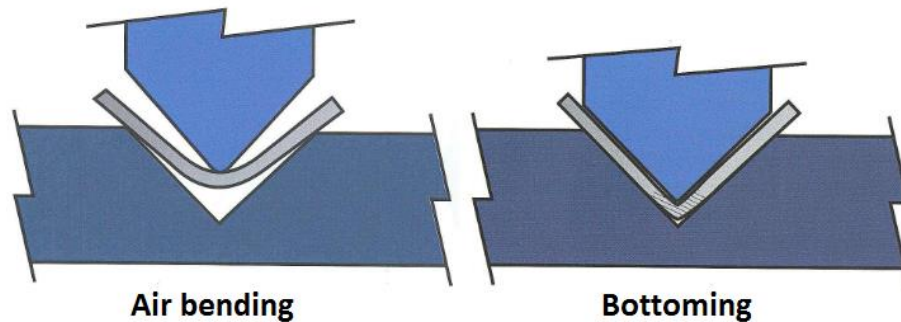
**Figure 10.** Prima Power eP-1030 series press brake (Prima Power 2013, p. 2).

The press brake can be operated hydraulically, mechanically or pneumatically. Pneumatic press brakes are rare and high – power machines are operated hydraulically. Hydraulic cylinders enable the adjustment of stroke and if high precision is required the operation is executed by using servo motors. Modern press brake machines are numerically controlled. (Matilainen et al. 2011, p. 240.)

Typically metal sheets are bent by using air bending or bottoming. Sometimes bending may be done by using elastic bottom tool. In air bending the metal sheet is pressed against bottom tool which has V-opening. The geometry of upper and lower tools does not affect the final geometry of the bent sheet which is dependent on material strength and material thickness. By using air bending the metal sheet can be bent to an angle lower than 90 degrees. The adjustment of the angle can be done by adjusting stroke length of the upper tool. (Matilainen et al. 2011, p. 241.)

Bottoming is also done by using V-opening tool as a bottom tool. The difference between bottoming and air bending is that in bottoming the upper tool is pressed against bottom tool and the metal sheet is left between the tools. The final shape of metal sheet is dependent on geometry of upper and lower tools. Plastic deformation of the sheet can be achieved by using bottoming but 3–5 times higher forces are required in comparison to air bending. The goal

in bottoming is to acquire high precision and rigid parts. Because of the requirement of higher forces and higher precision bottoming is more suitable for higher volume and less than 2 mm thick sheet parts. Principles of air bending and bottoming are presented in figure 11. (Matilainen et al. 2011, p. 241-242.)



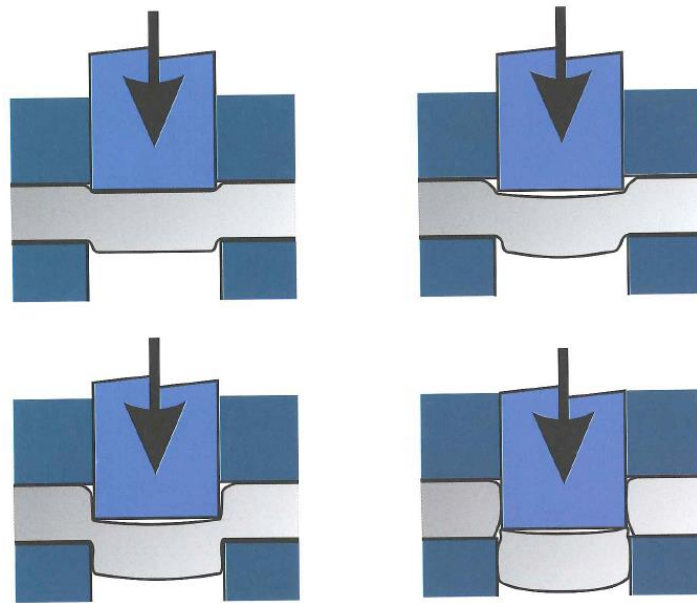
**Figure 11.** Principles of air bending and bottoming (Adapted from: Matilainen et al. 2011, p. 241).

Bending against elastic bottom tool is similar to bottoming, but instead of hard bottom tool an elastic cushion is used. Using of elastic bottom tool enables bending of more complex geometries and protects the workpiece from scratches. The material for bottom tool must be chosen correctly, because soft tool requires longer stroke length and hard tool requires higher force. Bending against elastic bottom tool is not precise method for bend lengths over 2 meters. (Matilainen et al. 2011, p. 242.)

### 2.6.2 Cutting Operations

Cutting of sheet metal is often the first step in manufacturing process of sheet metal parts and there are different methods to cut metal sheets. As a result of cutting the workpiece may be straight or cut into a shape, depending on cutting method. (Matilainen et al. 2011, p. 142) This paragraph will cover principles of two cutting methods: punching and laser cutting.

Punching is mechanical cutting process which can be used to cut closed shapes in metal sheets. The required shape is punched in metal sheet by using a punch, which is pressed against a die. The principle of punching is shown in figure 12.

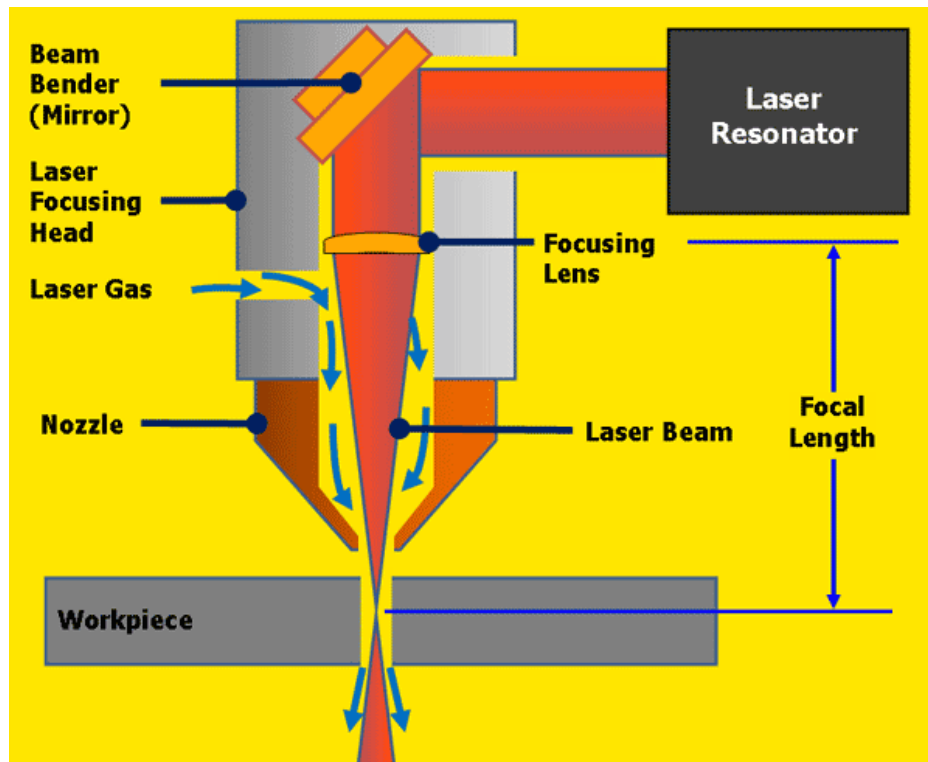


**Figure 12.** Principle of punching (Matilainen et al. 2011, p. 180).

As can be seen from figure 12 the punching is based on deformation of the material. First the material is deforming elastically after which it starts to deform plastically. When fractures caused by punch and die are linked the material is cut. (Matilainen et al. 2011, p. 179.)

Use of eccentric punching machines is traditional way to manufacture punched products but commonly used punching machines are hydraulic or servo controlled. Manufacturable sheet sizes are affected by the structure of the machine and useable tooling. Typical range of pressing force is 150-600 kN and typical material thickness range is 0.5-8 mm. Depending on a punching machine type metal sheets may be also formed and marked. (Matilainen et al. 2011, p. 180.)

Laser cutting can be used to cut different materials including steel and it is fast process with high quality cut which does not require machining after the cut is made. In laser cutting process laser beam is used to melt or vaporize material and flow of gas which is parallel to the beam is used to blow excessive material out. Figure 13 illustrates working principle of laser cutting.



**Figure 13.** Principle of laser cutting process (ESAB 2013).

The laser gas in cutting process can be oxygen or inert gas such as nitrogen. Oxygen is used in cutting carbon steels and inert gas can be used in cutting any metals and some polymers and ceramics. Sharp edges, small holes and other shapes that require precise cut may be problematic when oxygen is used as laser gas. When inert gas is used in cutting process the challenge is burr which is formed on the bottom side of the sheet if cutting parameters are not set correctly. (Matilainen et al. 2011, p. 159.)

Laser cutting machine can be CO<sub>2</sub>-laser or Nd: YAG (Neodymium Yttrium-Aluminum-Garnet) laser. The majority of machines used are CO<sub>2</sub>-lasers that are based on mirror and lens optic technology. In Nd: YAG-lasers controlling the laser beam is easier than in CO<sub>2</sub>-lasers because the beam is transferred via optical fiber and 3D-cutting is more flexible than in CO<sub>2</sub>-lasers. (Matilainen et al. 2011, p. 161-162) An example of modern laser cutting machine is shown in figure 14. As seen from figure 14 modern laser cutting machines can perform 3D cutting and can have two independent cutting heads.



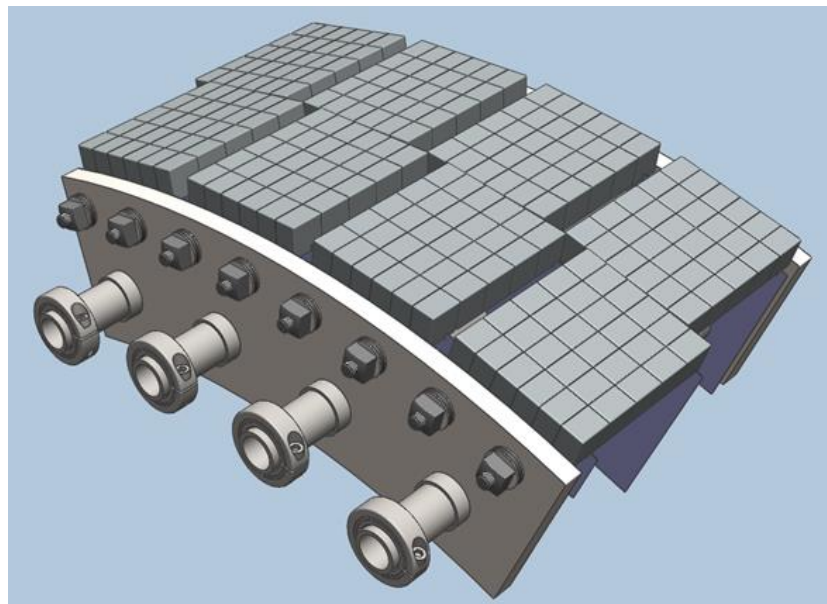
**Figure 14.** Prima Power Laserdyne 606 D 3D dual laser processing machine (Prima Power 2017, p. 22).

### 3 RESEARCH RESULTS

In this chapter results of performed tests and analyses are presented. For each presented element the function of the element and focus of the study are presented. Binding rods are observed from the perspective of binding force and wheel face lamination clamps are discussed from the perspective of clamping force. The clamping force was calculated analytically and determined by using FE analysis. For balsa wood spacers the manufacturing methods are discussed and non-oriented electrical steel laminations are observed from the perspective of coatings. The last discussed element is torsion box which is used for assembly process of wheel face stacks. The building process of the torsion box is presented and design of wheel face assembly tool is discussed from the perspective of systematic machine design and DFMA.

#### 3.1 Binding rods for rotor and stator segments

In the structure of LWLC machine fiberglass vinyl ester rods were planned to be used to bind electrical steel laminations into segments as shown in figure 15. The advantages of vinyl ester material consists of fatigue resistance, toughness and chemical resistance (Wallenberger & Bingham 2010, p. 151). Additional advantages are low conductivity and transparency to electromagnetic waves (Fiberglass Studs & Nuts 2017).



**Figure 15.** Fiberglass vinyl ester binding rods (with square nuts) used to bind laminations.

The advantages of fiberglass vinyl ester rods were suitable for use in LWLC machine, especially because of low conductivity and transparency to electromagnetic waves. A stud bolt was tested according to manufacturer's installation torque recommendation in order to establish its binding force and to observe any possible damages the bolt may suffer when tightened. The results of the test are discussed in the following paragraph.

### 3.1.1 Binding Force

For testing the binding force of fiberglass vinyl ester stud bolt joint, a 3/8-16 UNC fiberglass vinyl ester stud bolt was used with two nuts made of thermoplastic, two steel washers and one Raymond Die spring (ST53250). The mentioned parts were assembled together as shown in figure 16.



**Figure 16.** Test assembly for fiberglass vinyl ester stud bolt.

The assembly shown in figure 16 was attached to a vise in vertical position, leaving one end free as shown in figure 17.



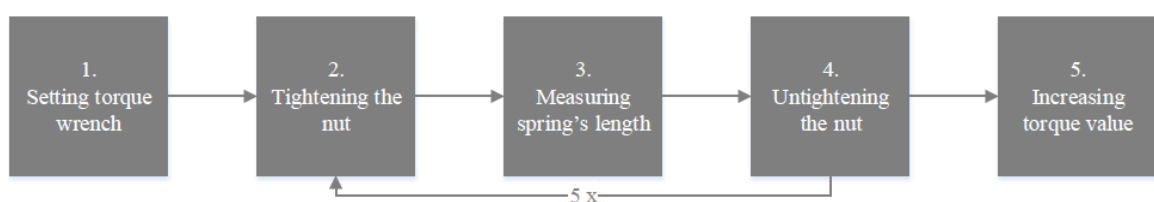
**Figure 17.** Bolt test assembly attached to a vise.

A torque wrench was used for applying torque to the nut at the free end of the bolt assembly. As the nut was turned in “closing” direction, the spring was compressed and the length of the spring was measured by using caliper. Measured length was used to calculate the binding force from the following equation:

$$F_{bind} = k_{spr}x_{spr} \quad (1)$$

In equation 1  $k_{spr}$  is spring constant 84 N/mm and  $x_{spr}$  is displacement of the spring which was established by subtracting measured length from the initial length of the spring.

The torque wrench was set to 1 Nm setting in the beginning of the test and increased by 1 Nm during the test, up to 6 Nm. For each value of torque five separate measurements were done before moving up to the next value of torque. Figure 18 illustrates the procedure of the test.



**Figure 18.** Steps 2, 3 and 4 were repeated five times before increasing torque value.

According to the information provided by the manufacturer of fiberglass vinyl ester stud bolts, Strongwell, the recommended maximum installation torque for 3/8-16 UNC bolt is 4 ft-lbs. which equals to 5.42 Nm, if the bolt is lubricated with SAE 10W30 oil (Strongwell, 2017). First test was done without lubrication and in second test graphite-based roller bearing grease was used on thread and the bottom of the nut.

In order to calculate the binding force average values were calculated for spring displacements at each value of applied torque. Average displacements of non-lubricated test and lubricated test and calculated forces are shown in table 1.

*Table 1. Average values of displacement of the spring and binding forces.*

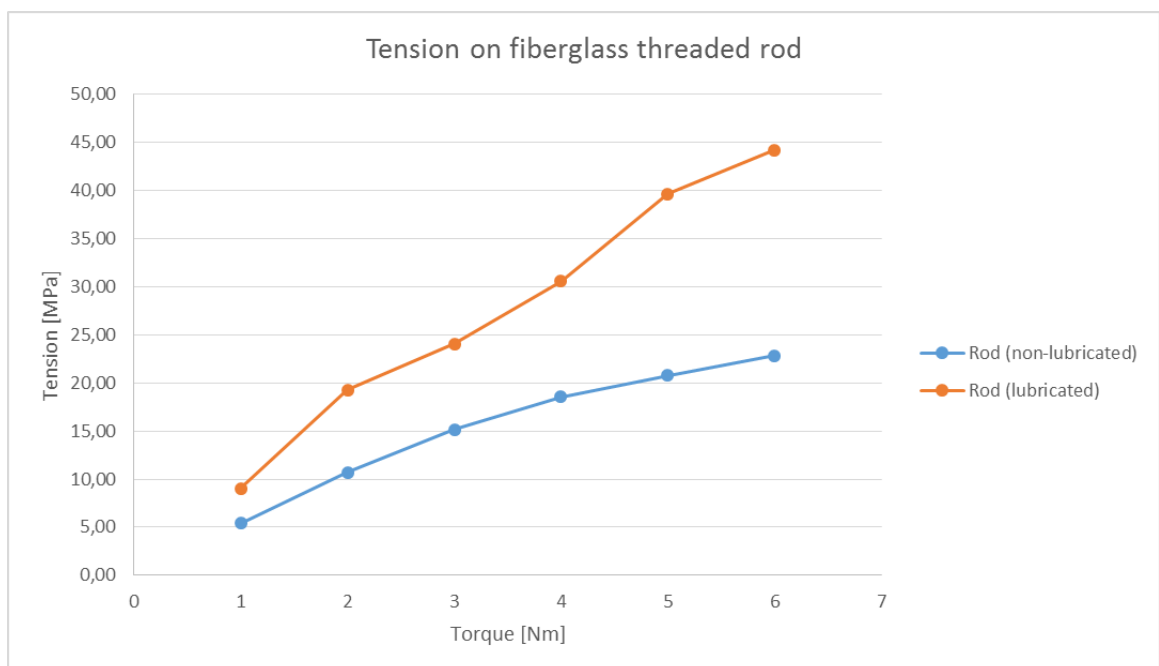
| Non-lubricated test |                |           |
|---------------------|----------------|-----------|
| Torque [Nm]         | Avg disp. [mm] | Force [N] |
| 1                   | 3,64           | 305,76    |
| 2                   | 7,20           | 604,80    |
| 3                   | 10,20          | 856,80    |
| 4                   | 12,50          | 1050,00   |
| 5                   | 14,00          | 1176,00   |
| 6                   | 15,38          | 1291,50   |
| Lubricated test     |                |           |
| Torque [Nm]         | Avg disp. [mm] | Force [N] |
| 1                   | 6,10           | 512,40    |
| 2                   | 13,00          | 1092,00   |
| 3                   | 16,20          | 1360,80   |
| 4                   | 20,60          | 1730,40   |
| 5                   | 26,70          | 2242,80   |
| 6                   | 29,80          | 2503,20   |

As seen from table 1 lubricated joint provided double the displacement compared to non-lubricated joint, which results in 48% higher binding force at 5 Nm and 6 Nm torque values. Result charts for displacements of 5 Nm and 6 Nm tests and displacement-force comparison chart can be found in appendix II.

For determination of tension in the stud bolt, the tension was thought as normal stress, which can be calculated using the following equation:

$$\sigma_{rod} = \frac{F_{bind}}{A_{rod}} \quad 2)$$

in which  $\sigma_{rod}$  is the tension of stud bolt and  $A_{rod}$  is cross-section area determined by using bolt's basic effective diameter. The basic effective diameter of used stud bolt was 0.3344 inches, which is 8.49376 mm (Tap Chart-UNC/UNF Threads, 2016). Figure 19 illustrates chart in which non-lubricated and lubricated test results for tension are shown for each value of applied torque.



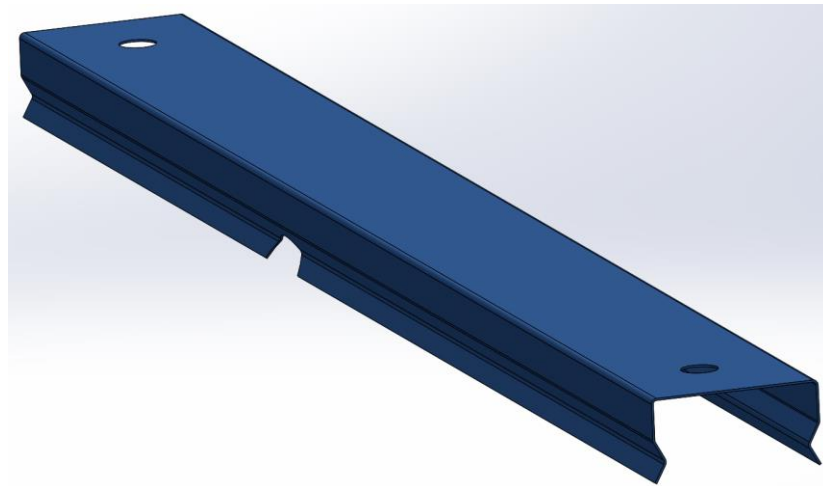
**Figure 19.** Torque-tension chart for non-lubricated and lubricated joint tests.

The difference between non-lubricated joint and lubricated joint can be seen from figure 19. As the result of lubrication by graphite-based roller bearing grease the tension of the stud bolt in lubricated joint is 48% higher than the tension in non-lubricated joint.

From the results of binding rod tests the binding force for manufacturer's recommended installation value of 5.42 Nm can be approximated to 2400 N. At 2400 N binding force the tension of the stud bolt can be estimated to be 42 MPa. During the tests the stud bolt and both nuts did not suffer major damages and withstood the recommended installation values.

### 3.2 Wheel face lamination clamps

As mentioned in paragraph 1.1 the LWLC machine is made of stacked sheet metal laminations which provides effective structural damping. Holding of wheel face laminations together was planned to be done by using clamping parts that work similarly to spring clamps. The proposed geometry for clamping part is shown in figure 20. Because of deformation of clamping parts when assembled on wheel face lamination stack, stainless spring steel was chosen as the material for clamping parts. Commonly stainless spring steel has high strength, which means the material will not be plastically deformed during the assembly (Sandvik 2003, p. 5).



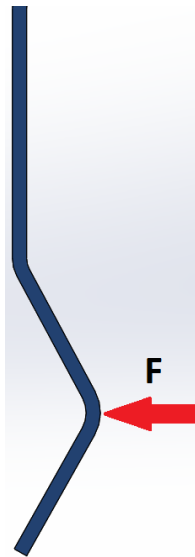
**Figure 20.** Wheel face lamination spring clamp.

Profile of proposed spring clamp was designed for 39 mm wide spoke of 750 kW machine's rotor wheel face. The gap between clamping surfaces was 35 mm, which meant each side of the clamp had to be displaced 2 mm in order to attach the clamp to the spoke. The 2 mm displacement distance was used in analytical calculations of the clamping force as required displacement.

#### 3.2.1 Clamping force

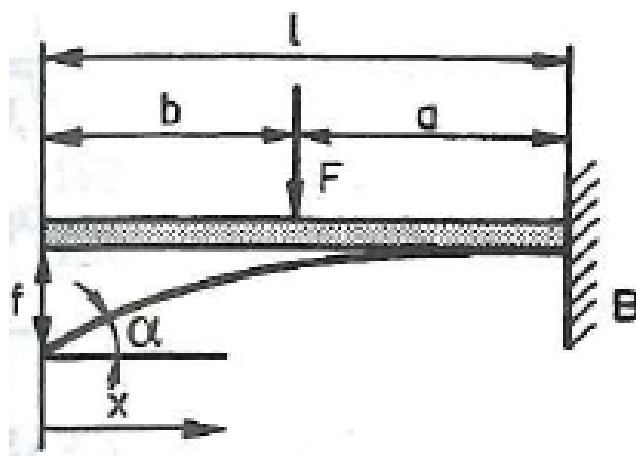
Calculation of clamping force was first done analytically in order to determine magnitude of the clamping force. After the calculation the spring clamp was exported to commercial FE software, Femap for further analysis. In order to calculate clamping force on one side of the spring clamp the clamp was considered as a beam which is fixed in one end and free in other

end and the load is not in the free end. Figure 21 illustrates the consideration made for analytical calculations.



**Figure 21.** Simplified model of spring clamp for calculation.

In the simplified model of spring clamp shown in figure 21 the upper end was considered as fixed and bottom end as free. The bend which can be seen in figure 20 was not taken into account in the calculation. The calculation was done by using equation of displacement of a beam which is fixed in one end as shown in figure 22. In figure 22 the fixed end of the beam is marked as  $B$ ,  $F$  is the load,  $a$  is the distance of the load from fixed end,  $b$  is the distance of the load from free end,  $l$  is the length of the beam,  $f$  is displacement of the free end and  $\alpha$  is displacement angle.



**Figure 22.** Loaded beam with one fixed end (Valtanen 2010, p. 409).

As can be seen from figure 22 the load on the beam is not in the free end, which was similar to the spring clamp. The equation for calculating the displacement of the free end according to Valtanen (2010, p. 409) is:

$$f_c = \frac{F_c a_c^3}{6E_c I_c} \left( \frac{3l_c}{a} - 1 \right) \quad (3)$$

In equation 3  $f_c$  is displacement of the free end,  $F_c$  is clamping load,  $a_c$  is distance of the load from fixed end,  $E_c$  is elastic modulus of the material,  $I_c$  is moment of inertia of the simplified clamp and  $l_c$  is total length of the simplified clamp. In order to calculate the clamping force equation 3 was modified to the following form:

$$F_c = \frac{6E_c I_c f_c}{(3l_c a^2 - a^3)} \quad (4)$$

As can be seen from figure 19 the spring clamp has slot on both sides which divides clamping surface in two surfaces. The surfaces were not symmetric as the slot was not in the middle. As a result two different moments of inertia were calculated in order to establish the clamping force of each clamping surface of the clamp. Table 2 shows calculated values of clamping force for shorter and longer surface of the spring clamp.

*Table 2. Calculated values of clamping force.*

|                    |         |         |
|--------------------|---------|---------|
| <b>0,5mm thick</b> | Long    | Short   |
| Width [mm]         | 254,631 | 172,631 |
| Force [N]          | 628,719 | 426,249 |
|                    |         |         |
| <b>0,8mm thick</b> | Long    | Short   |
| Width [mm]         | 254,631 | 172,631 |
| Force [N]          | 2575,0  | 1746,0  |

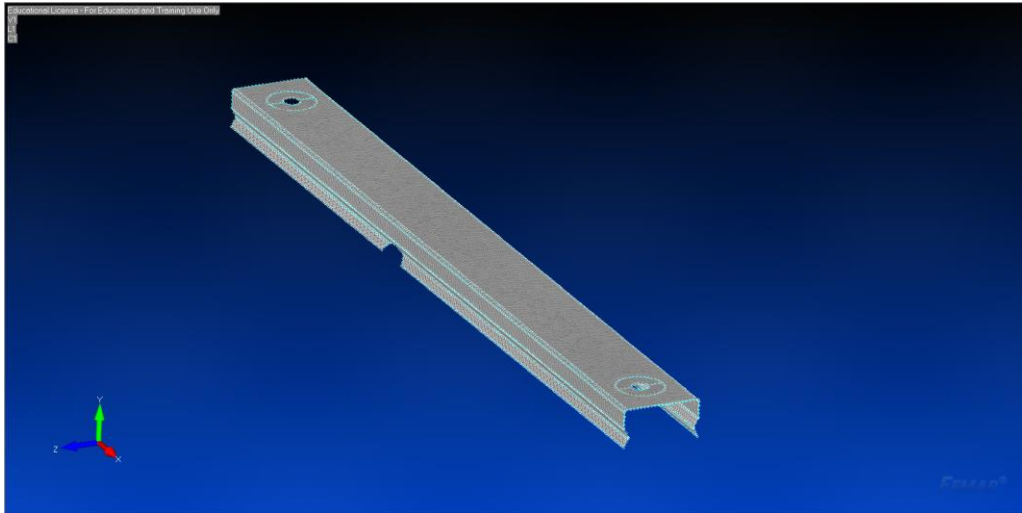
As can be seen from table 2 there were two different material thicknesses proposed for spring clamps: 0.5 mm and 0.8 mm. The calculation procedure used can be found in appendix I.

The model of spring clamp was exported to Femap-software, version 11.2.1 for static analysis. NX Nastran V10.2 was used solver in analyses. The exported 3D model was converted into mid-surface model in order to simplify the analysis. Table 3 shows the set-up made for static analysis in Femap.

*Table 3. Set-up for static analysis in Femap.*

| <b>Set-up for Femap analysis</b> |            |
|----------------------------------|------------|
| <b>Material:</b>                 |            |
| Elastic modulus [MPa]            | 200000     |
| Poisson's ratio                  | 0,3        |
| <b>Mesh:</b>                     |            |
| Element type                     | Plate      |
| Element shape                    | Triangular |
| Number of elements               | 21912      |
| <b>Loads:</b>                    |            |
| Long edge [N]                    | 630        |
| Short edge [N]                   | 426        |
| <b>Constraints:</b>              |            |
| Bolt joint                       | Fixed      |

Elastic modulus was set according to stainless steel EN 1.4301's properties (Outokumpu 2015). For mid-surface model linear plate elements were used. The element type was marked in Nastran solver as CTRIA3. The fixation of clamp was done by adding offset curves around bolt holes to represent washers and fixing the surfaces under the washers. With used constraints only the area under washers was fixed and the rest of construction may have deformed freely. Forces were applied to shorter and longer clamping surfaces according to values presented in table 3. The Femap model for analysis is shown in figure 23.



**Figure 23.** Mid – surface model of spring clamp.

Study of results was concentrated on translation of spring clamp's sides but stresses were also taken into account in order to confirm that they will not exceed the yield strength of the material. Results of first static analyses for both material thicknesses are presented in table 4.

*Table 4. Results of first static analyses.*

|                        |       |
|------------------------|-------|
| <b>0,5 mm thick</b>    |       |
| Total translation [mm] | 8,417 |
| Von Mises stress [MPa] | 1735  |
|                        |       |
| <b>0,8 mm thick</b>    |       |
| Total translation [mm] | 8,504 |
| Von Mises stress [MPa] | 2739  |

Table 4 shows that total translations of both material thicknesses are 52% higher than initially required total translation of 4 mm. Also Von Mises stresses were higher than tensile strength of the material. According to standard SFS-EN 10088-2 (2014, p. 41) the tensile strength of 1.4301 cold rolled sheet is 540-750 MPa. The resulted peak stresses achieved from Femap static analyses were 131% higher for 0.5 mm thickness and 265% higher for 0.8 mm thickness compared to tensile strength of the material.

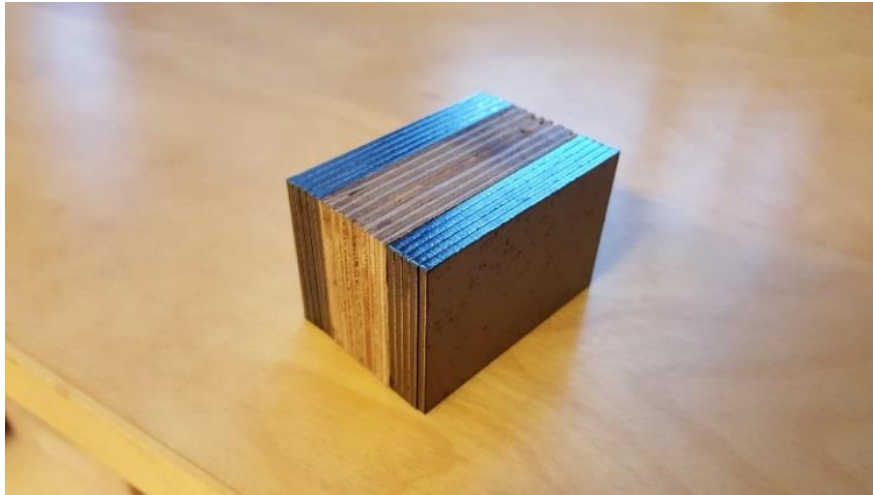
For the second static analysis run all the forces were lowered by half from initial values. Fixation of the spring clamp was kept the same as in first analysis. Also the number and shape of elements was the same as in first analysis. Second analysis run results are presented in table 5.

*Table 5. Results of second static analysis.*

|                        |       |
|------------------------|-------|
| <b>0,5 mm thick</b>    |       |
| Total translation [mm] | 4,215 |
| Von Mises stress [MPa] | 869   |
|                        |       |
| <b>0,8 mm thick</b>    |       |
| Total translation [mm] | 4,253 |
| Von Mises stress [MPa] | 1370  |

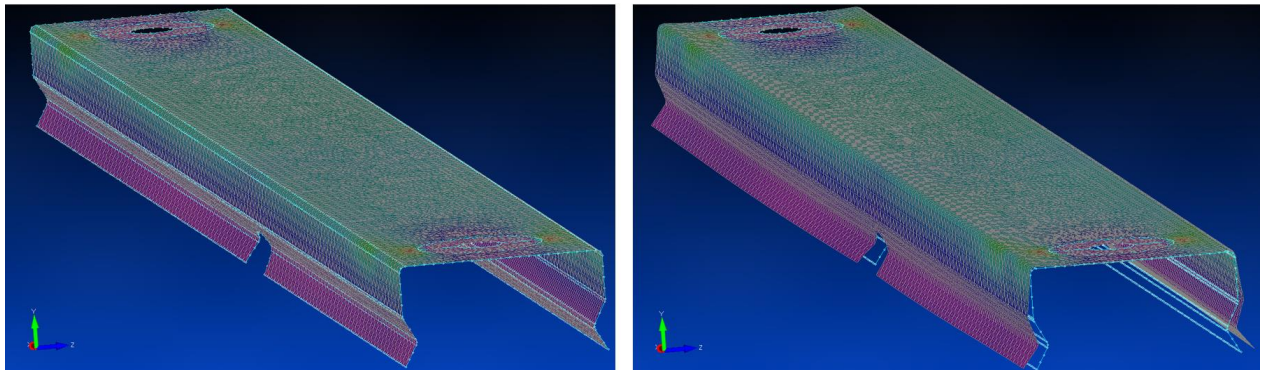
As can be seen from table 5 decreasing the forces by half affected total translation and Von Mises stress. The results of second static analysis show that total translation achieved from Femap analyses is 5% higher than initial 4 mm. The peak stresses in second analyses were half of the values from first analyses. Peak Von Mises stress of 0.8 mm thick spring clamp still exceeded material's tensile strength and overall in clamp the stress was in the range of 540–750 MPa. For 0.5 mm thick clamp the peak stress was 16% higher than material's tensile strength. Peak stresses in spring clamp were local stresses. Overall in the structure of 0.5 mm thick clamp Von Mises stress did not exceed tensile strength of stainless steel EN 1.4301. According to Femap analyses for both 0.5 mm and 0.8 mm thick spring clamps the most suitable solution for LWLC wheel face lamination clamp was 0.5 mm thick clamp.

In order to evaluate results from analytical calculations and Femap analyses and also to confirm spring clamp's clamping capability and durability during the assembly a test samples were made. Sample pieces were not full length clamps but instead 50 mm long pieces without any holes or slots. First sample was made of 0.8 mm thick stainless spring steel. The sample clamp was installed on test assembly which represented wheel face spoke. The test assembly is shown in figure 24.



**Figure 24.** Test assembly representing wheel face spoke.

As can be seen from figure 24 test assembly consisted of ten sheet metal parts and plywood piece. The test clamp was installed on the test assembly without noticeable damage and clamping force was high enough to keep the stacked parts together. Also the deformation of assembled clamp was observed and it was similar to the deformation shown in figure 25.



**Figure 25.** Clamp without deformation on the left and deformed clamp on the right.

After testing 0.8 mm thick clamp next sample clamps were ordered. New sample clamps were 0.5 mm thick and they were made in full length with slots on both sides. The installation of full size clamps was made on real-size rotor wheel face of 750 kW machine. After the installation 0.5 mm was considered as suitable thickness for wheel face lamination spring clamps as they provided suitable clamping force and kept wheel face stack parts together.

### 3.3 Balsa wood spacers

Balsa wood spacers were planned to be used in LWLC machine between sheet metal laminations as can be seen in figure 1 in paragraph 1.1. The main reason for using balsa wood spacers was maintaining the gap between two wheel face lamination stacks. Another reason for using balsa was its light weight, which was suitable for light-weight structure of LWLC machine.

Balsa wood is light material with density values of 40-380 kg/m<sup>3</sup> and density of wood solid is approximated to be 1500 kg/m<sup>3</sup>. Relative density of balsa wood can be presented as ratio of density and wood solid density. As a result relative density of balsa wood may vary in the range of 0.027-0.26. The relative density values show that volume of empty space in balsa wood's cellular microstructure is high. Balsa wood has high strength and axial stiffness, which gives it excellent energy absorption characteristics. (Silva & Kyriakides 2007, p. 8686) Energy dissipation capacity of balsa wood can be compared or considered better than most composite tubes with fiber reinforcement. The range of energy dissipation of balsa wood is 30-90 kJ/kg. Excellent capacity of energy dissipation is result of balsa wood's natural microstructure, tubular honeycomb geometry. (Vural & Ravichandran 2003, p. 2156-2157)

The manufacturing method had to be chosen for manufacturing balsa wood spacers because balsa was provided in 1" thick sheet form. There were three methods to cut balsa parts from sheet: CNC milling, laser cutting and water jet cutting. Each method was observed from the perspective of cutting balsa in order to find advantages and disadvantages. Table 6 shows advantages and disadvantages that were taken into account when useable method was chosen.

Table 6. Advantages and disadvantages of three cutting methods.

|                     | <b>CNC milling</b>   | <b>Laser cutting</b>    | <b>Water jet cutting</b>                              |
|---------------------|--|-------------------------|---|
| <b>Advantage</b>    | - Clean cut<br>- Fast  | - Precise cut<br>- Fast | - Precise cut<br>without<br>burning the material      |
| <b>Disadvantage</b> | - With wrong<br>cutting<br>parameters<br>may damage<br>the balsa | - May burn balsa        | - Balsa may expand<br>after the contact<br>with water |

The most common cutting method of presented three was laser cutting. Disadvantage of laser cutting was the possibility that cut surface of balsa may be burnt, which was not acceptable. Water jet cutting was considered as precise method which does not burn the balsa. The disadvantage of water jet cutting was possible expansion of balsa after the contact with water. Expanded balsa parts would not be the correct size for LWLC machine's wheel face. CNC milling was the most suitable method because it can provide clean cut without burning or deforming the parts. The only disadvantage of CNC milling was possible damage to balsa parts, especially near corners.

After the selection of manufacturing method for balsa wood spacers was done, two sample parts were made. Cutting parameters were first tested on a piece made of pine before cutting the balsa. After the parameters were set first sample piece of balsa part was cut from small sheet as shown in figure 26.



Figure 26. Cutting process of balsa wood part.

Sample pieces were planned to be 19 mm thick, which meant the initial thickness of parts, 25.4 mm (1") had to be reduced. After two sample parts were cut they were put into grinding machine in order to grind them in correct thickness. Both parts withstood cutting and grinding processes without any damage. The accuracy of cut parts shown in figure 27 was considered good.



**Figure 27.** CNC cut balsa spacers for rotor and stator rims.

As can be seen from figure 27 balsa wood sample parts were rim pieces for rotor and stator. Presented parts were made because their geometry was more complex than of balsa parts for spokes. Further development of the balsa wood spacers resulted in two different thicknesses. For rotor parts new thickness was 16 mm and for stator parts 22 mm.

### 3.4 Non-oriented Electrical Steel Laminations

Non-oriented electrical steel, also known as silicon electrical steel or transformer steel is used in stack form in electrical appliances, such as electric motors, generators or transformers. It is produced using iron – silicon (Fe-Si) or iron-silicon-aluminum (Fe-Si-Al) alloys. Non-oriented electrical steel is base material for electrical appliances because of its electrical energy transmitting and distribution properties. For such appliances requirements for the steel include high induction and permeability and low magnetic losses. Non-oriented electrical steel is supplied in two forms: fully-processed grades and semi-processed grades. Fully-processed grades are in finished condition and have magnetic properties defined in standard EN 10106. Semi-processed grades are not in finished condition, which means the

user has to perform final annealing treatment in order to achieve required magnetic properties. In terms of manufacturing non-oriented electrical steel can be made in the form of cold-rolled sheets or strips and supplied in stacks (sheet form) or coils (strip form). Commonly used thicknesses for non-oriented electrical steel sheets or strips are: 0.35 mm, 0.5 mm, 0.65 mm and 1 mm. (Petrovič 2010, p. 317.)

### 3.4.1 Coatings

The use of electrical steel laminations in electrical appliances result in iron losses and eddy current in laminations. The eddy current loss can be reduced in the core by insulating electrical steel laminations, which leads to eddy currents being constrained to individual laminations. (Lindenmo, Coombs & Snell 2000, p. 79.) According to Lindenmo et al. (2000, p. 79) the following items are included in selection process of suitable coating:

- “insulation resistance
- punchability properties
- corrosion resistance properties
- weldability
- heat resistance
- stacking factor
- chemical resistance
- burn-out characteristics
- resistance to compression
- coating thickness
- surface roughness
- scratch resistance properties”

During the process of making laminations some burr may be left on the laminations, which may lead to short circuits and therefore to major failure of the machine. This risk can be eliminated by grinding the burr off or increasing the thickness of the coating layer. (Lindenmo et al. 2000, p. 79.)

A range of different coatings has been developed in order to satisfy the requirements of different electrical steel applications. The coatings are divided in six types: C0, C1, C2, C3, C4 and C5. Organic, mixtures of organic and inorganic and fully organic coatings are included in this range of coatings. Because of different properties of the coatings, the

selection of a coating is often a compromise as on some occasions single coating cannot fulfill the requirements. In order to fulfill the requirements four coatings were developed by EES (European Electrical Steels): SURALAC 1000, SURALAC 3000, SURALAC 5000 and SURALAC 7000. These SURALAC coatings cover the wide range of coating properties (Lindenmo et al. 2000, p. 81). Properties of SURALAC coatings are presented in table 7.

Table 7. Properties of SURALAC coatings (Adapted from: Cogent 2016, p. 15).

| Designation                              | SURALAC 1000                | SURALAC 3000                | SURALAC 5000 | SURALAC 7000 |
|--|-----------------------------|-----------------------------|--------------|--------------|
| Type                                     | Organic                     | Organic with fillers        | Semi-organic | Inorganic    |
| Classification                           | C3                          | C6                          | S3           | C5           |
| Thickness range / side [μm]              | 0,7 - 6                     | 3,5 - 6                     | 0,7 - 1,2    | 0,7 - 3,5    |
| Standard thickness [μm]                  | 2,5                         | 6                           | 1,2          | 1,5          |
| Temperature capability in air [°C]       | 180                         | 180                         | 200          | 270          |
| Temperature capability in inert gas [°C] | 450                         | 500                         | 500          | 850          |
| Burn-out repair                          | -                           | Possible                    | -            | Possible     |
| Chemical resistances:                    |                             |                             |              |              |
| Stamping lubricants                      | Yes                         | Yes                         | Yes          | Yes          |
| Transformer oils                         | Yes                         | Yes                         | Yes          | Yes          |
| Freon                                    | Yes                         | Yes                         | Yes          | Yes          |
| Weldability                              | Special techniques required | Special techniques required | Excellent    | Good         |
| Punchability                             | Excellent                   | Moderate                    | Excellent    | Good         |
| Insulation resistance:                   |                             |                             |              |              |
| Ω*cm <sup>2</sup> / lamination           | 100                         | > 200                       | 20           | 50           |
| Amperes / side                           | 0,06                        | < 0,03                      | 0,25         | 0,11         |

In table 7 weldability, punchability and insulation characteristics are shown for standard thicknesses.

In LWLC machine the electrical steel stacks were not assembled by welding. Instead of welding laminations together fiberglass bolts were used to provide necessary binding force. In such application individual laminations may slide on top of another laminations. In order

to prevent sliding the laminations must have had coating with high friction. The establishment of friction was done by ordering sample pieces shown in figure 28 from a manufacturer of electrical steel laminations.



**Figure 28.** Sample pieces of three different coatings.

The sample pieces shown in figure 28 were coated with three different coatings: “glue”, SURALAC 5000 and SURALAC 7000. There were two sample pieces of each coating. Friction between sample pieces was tested by pushing two pieces together by hand and moving hands in opposite directions. Suitable coating was determined by sensing which sample pieces were the most difficult to move while pushed together.

According to table 1 SURALAC 5000 and SURALAC 7000 were the most suitable coatings because of their higher temperature capabilities. After testing the sample pieces SURALAC 5000 and SURALAC 7000 were discovered to be superior to “glue” in terms of friction. After eliminating “glue” coating because of its low friction SURALAC 5000 and SURALAC 7000 coatings were compared using the same method as in first test. Friction of both coatings was acceptable but SURALAC 7000 samples were harder to move, and it was considered that SURALAC 7000 coating has higher friction compared to SURALAC 5000.

### 3.5 Torsion Box

To find challenges and suitable assembly methods for assembly phase of LWLC machine a prototype wheel face of 750 kW machine's rotor was built. The prototype wheel face was not only used to establish methods and procedures of assembly but also to test spring clamps and balsa wood spacers. During the first assembly of wheel face prototype laminations and balsa wood spacers were assembled horizontally. Laminations were fixed with four bolts and balsa wood spacers were fixed with clevis pins and stud bolts. For spring clamp installation the wheel face was lifted to vertical position as shown in figure 29.

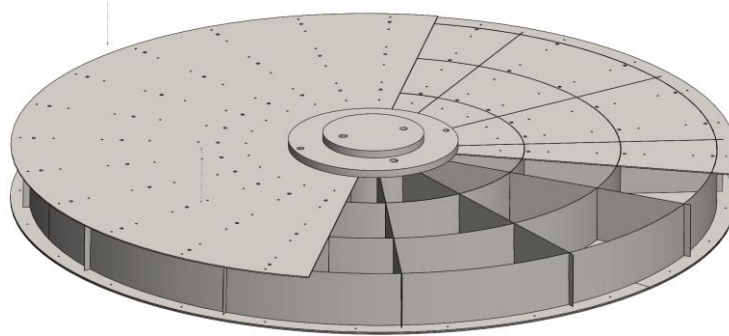


**Figure 29.** Assembled prototype of rotor wheel face of 750 kW machine.

The first assembly of prototype wheel face provided vital information for improvements of assembly process. The whole assembly procedure was decided to be done horizontally, not vertically as shown in figure 29. Horizontal assembly was easier in terms of aligning wheel face laminations, installing balsa wood spacers and preventing sagging of laminations.

For realizing horizontal assembly process a flat surface which could be able to support the whole diameter of wheel face laminations was required. This requirement was realized by building a torsion box. The torsion box was designed as round table with circular and radial walls inside to provide resistance to torsion and keep table surface flat. The diameter of torsion box was designed to support rotor wheel face of 750 kW LWLC machine, which is

in same size range with stator wheel face of 500 kW LWLC machine. The 3D model of proposed torsion box is shown in figure 30.



**Figure 30.** Structure of the torsion box.

The torsion box was designed to be built using sheet metal parts as can be seen from figure 30. Bottom and top layers were made of 3 mm thick sheet metal and circular and radial walls were made of 1 mm thick sheet metal. The middle hub shown in figure 29 was not made for testing of 750 kW machine's rotor wheel face assembly. Top and bottom 3 mm sheet disks were made from two halves because of the size limits of laser cutting machine.

Building of the torsion box was done on top of platform made of 108 mm OD (Outer diameter) steel pipes. Pipes were leveled before the beginning of building process to ensure horizontal position of the torsion box. First step was to attach segmented sheet parts to bottom plates. For attaching 3 mm thick segmented sheet parts rivet pins were used. In second step 1 mm thick circular and radial walls were installed in the slots of segmented plates as shown in figure 31.



**Figure 31.** Installed 1 mm thick circular and radial walls.

In third step upper segmented plates were installed. Installing of upper segmented 3 mm plates proved to be challenging because 1 mm walls did not fill in the slots without additional use of force. After the upper segmented plates were installed, in fourth step top surface plates were installed and attached to upper segmented plates by using rivet pins. In the last step torsion box bottom and top plates were bound together with carriage bolts.

### 3.5.1 Wheel Face Assembly Spacer Tools

A spacer tool between torsion box top surface and wheel face stack was required in order to provide necessary gap for clamp installation. Planning of spacer tool started with information gathering and discussion with people involved in the project. After necessary information of requirements was gathered, a requirement list shown in figure 32 was made.

| Ivan Baulin |  | Requirements list<br>for wheel face assembly spacer tool  | 28.2.2017   |
|-------------|--|---|-------------|
| Changes     | D / W  | Requirements  | Responsible |
| 28.2.2017   |  | Geometry:   | Ivan Baulin |
|             | W  | Height = 40 mm  |             |
|             | D  | Contact surface with wheel face = max. $\varnothing$ 5 mm |             |
|             | D  | Space for the magnet = min. $\varnothing$ 20 mm           |             |
|             | W  | Clearance for clamps                                      |             |
|             |  |   |             |
|             |  | Kinematics:   |             |
|             | W  | Free positioning on torsion box surface                   |             |
|             | D  | Zero movement during the assembly process                 |             |
|             | D  | Detachable from torsion box after the assembly            |             |
|             |  |   |             |
|             |  | Forces:   |             |
|             | D  | Withstandable load for one tool = 35 N                    |             |
|             | W  | Vertical load orientation                                 |             |
|             |  |   |             |
|             |  | Material:   |             |
|             | D  | Strong material to support wheel face                     |             |
|             |  |   |             |
|             |  | Safety:   |             |
|             | D  | No sharp objects  |             |
|             | W  | Good surface quality                                      |             |
|             |  |   |             |
|             |  | Production:   |             |
|             | W  | Made by turning process                                   |             |
|             |  |   |             |
|             |  | Assembly:   |             |
|             | D  | Magnet installed on the bottom of the tool                |             |
| W           | Enough space to detach the magnet if necessary |   |             |
|             |  |   |             |
|             | Costs:   |   |             |
| D           | Maximum total price of the tools = 300 €       |   |             |

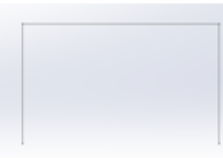


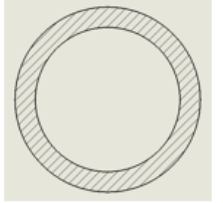

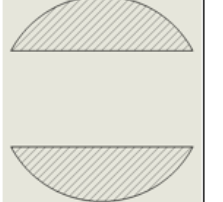


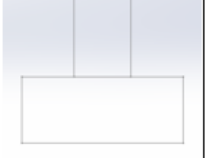
**Figure 32.** Requirement list for spacer tool.

The requirement list shown in figure 32 was made for simple tool which did not have complex sub-assemblies or moving parts. As a result refining of requirement list was considered not necessary and it was used as it is shown in figure 31. In the requirement list demands were marked with letter “D” and wishes with letter “W”.

Geometry demands were set to enable the installation of magnet and to ensure good contact between the tool and the wheel face stack. Height was set as a wish because it was dependent on the height of central hub of the torsion box. During the assembly process zero movement of the assembly tool was considered as a demand. Also detaching of the tool from torsion box was important in order to reposition tools if the size of wheel face laminations would change.

Each assembly tool was considered to be loaded vertically. The demand for durability of the tool was calculated from the weight of one wheel stack. As a result the demand for each tool was to withstand load of 35 N. The material of the assembly tool was not specified and demand for it was only the ability to support wheel faces. Safety of workers was taken into account by setting demand for no sharp edges. Also the assembly of the tool was taken into account and the only demand was the possibility to attach magnet on the bottom of the tool. All wishes presented in the requirement list were taken into account after all demands were satisfied.

After the requirement list was done and demands were acknowledged a classification scheme was formed. The classification scheme shown in figure 33 was used to aid the selection of suitable geometry of the spacer tool.

| Subfunction / Solution |               | a   | b  | c   |
|------------------------|---------------|---|--|---|
| 1                      | Head geometry |  |  |  |
| 2                      | Magnet slot   |  |  |  |
| 3                      | Body geometry |  |  |  |

**Figure 33.** Classification scheme of spacer tool.

The spacer tool was divided into three subfunctions: head geometry, magnet slot and body geometry. For each subfunction three possible solutions were created. The combination of subfunctions and solutions was done as explained in paragraph 2.3 by choosing one solution for each subfunction. As a result of combination the proposed spacer tool consisted of following combinations: 1a, 2c, 3a. A prototype spacer tool shown in figure 34 was built for observation of functionality of the tool.



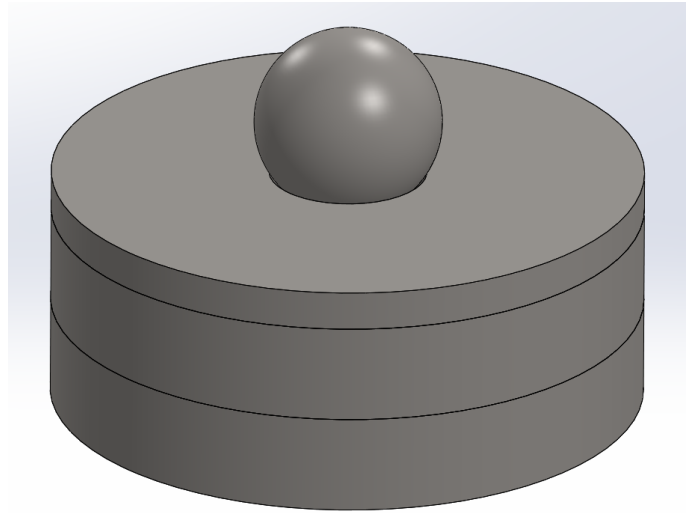
**Figure 34.** Prototype of spacer tool for wheel face assembly.

The prototype spacer tool was manufactured by using turning operation and slot for magnet was machined by face milling. First step of observation was installing the magnet in the slot and testing of attachment of the tool to the steel surface. The air gap between magnet and steel surface was 2 mm, which was the same as thickness of the magnet. The spacer tool was firmly attached to the steel surface while keeping its movement along the surface possible. Removing of the spacer tool was challenging if pulled straight up but possible by lifting its one end before pulling up.

Second step of observation concentrated on geometry of the tool and geometry of its head. The cone geometry of the tool was achieved by turning operation but it was considered expensive solution, because of large amount of excessive material. Reduction of excessive material was proposed to be done by keeping the diameter of the tool the same until the top area, where the shaft could have been machined thinner. This solution can be seen from figure 32 as combination 3b. Also the head of the tool required review because it was considered challenging to keep the top surface similarly flat in every tool out of 72. Instead of flat top surface it was proposed that it should be round. Round surface would provide similar contact between torsion box surface and wheel face stack. As a result solutions 1b and 1c were considered more suitable for head geometry of the spacer tool.

The proposed geometry of spacer tool shown in figure 33 fulfilled all demands presented in requirement list except the safety and the costs. The machined slot for magnets left sharp edges on the outer diameter of the spacer tool, which may damage worker in assembly process. Also because of the high amount of excessive material in turning operation manufacturing of one piece was considered expensive. Machining of magnet slot was also an additional process which required the change of tool. Taking into account presented issues the spacer tool prototype was not considered DFMA-friendly.

In order to fulfill all the demands from the requirement list and to make the spacer tool more DFMA-friendly, a new geometry was proposed. In new geometry the following combinations of classification scheme could be noticed: 1c, 2a, 3b. The proposed design of new spacer tool is presented in figure 35.

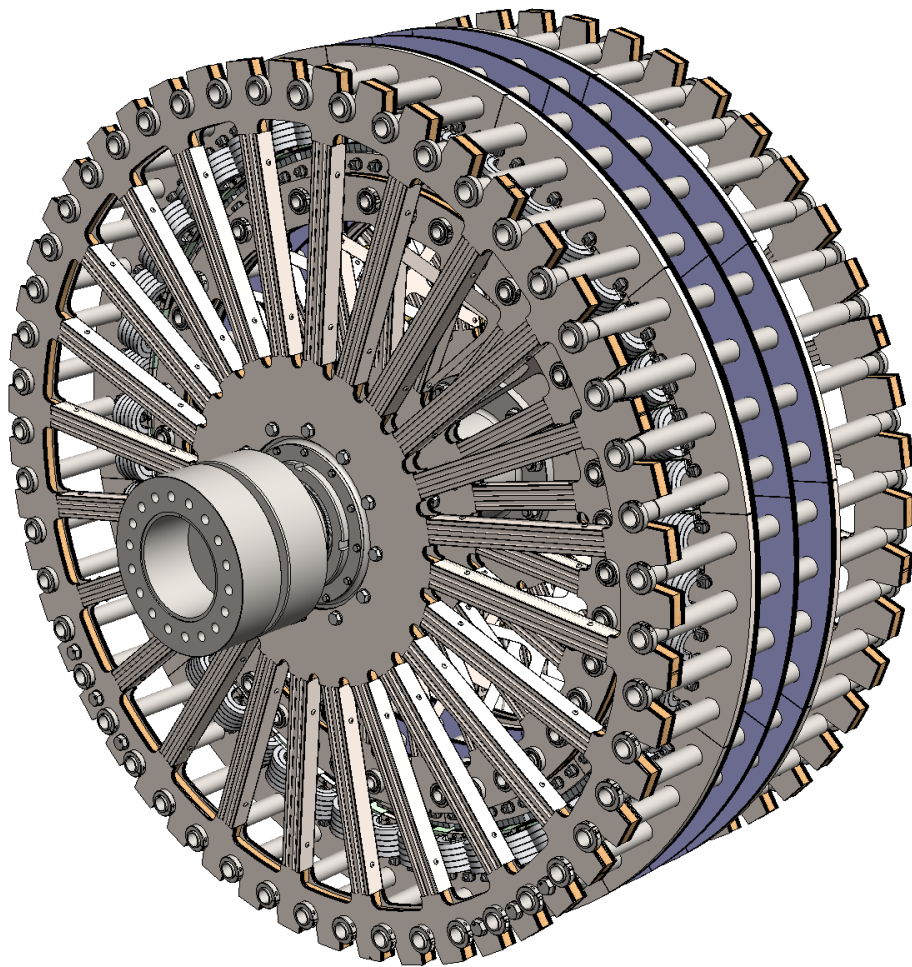


**Figure 35.** Updated geometry of the spacer tool.

The updated design of spacer tool consisted of a ring, disk, washer and bearing ball. Ring and disk pieces were planned to be cut by laser from 4 mm thick sheet metal and glued together. The washer was also planned to be glued on top of the disk and bearing ball to be inserted in the hole of the washer. The updated spacer tool design was considered more DFMA-friendly as the same material thickness and one manufacturing process could have been used for 50 % of the parts. Also the cost of new spacer tool was considered lower than of first design, especially when making of 72 pieces was taken into account. All 72 rings and disks could have been cut from the same sheet metal piece with low amount of excessive material. The updated spacer tool also fulfilled all the demands of requirement list as it did not have sharp edges, making the design safer for workers to handle.

## 4 CONCLUSIONS

The design of structural elements of LWLC machine was done using calculations, FE analyses and practical experiments. Initial design of parts presented in this thesis was modified to ensure the functionality of the parts. During the design process and performed tests new elements for assembly were created as a result, such as torsion box and wheel face assembly spacers. Modification of structural elements of LWLC machine resulted in new structure design which can be seen in figure 36.



**Figure 36.** Modified structure of LWLC machine.

The most noticeable change in the structure of LWLC machine compared to figure 1 is new design of wheel faces. In old design shown in figure 1 spokes are slanted. New design of LWLC machine has straight spokes, which gives it same stiffness in both rotating directions.

Good stiffness in both rotating directions enable the use of LWLC machine in industrial applications that may require direction changes in rotation, such as shredders and mixers. The LWLC machine can also be used as replacement for induction motor – gearbox combination in wind turbine nacelle.

Figure 36 also shows coupling mechanism at the end of the shaft. The coupling mechanism is keyless, which means it relies on the friction between the shaft and the surface of the inner ring of the coupler. Presented coupling unit can be used in shaft-to-shaft connections. Other changes in the new structure of LWLC machine are wheel face lamination clamps' geometry and thicknesses of balsa wood spacers. Components of LWLC machine and its assembly that were studied in this thesis are presented further in this chapter.

The assembly process of LWLC machine's wheel faces was decided to be done horizontally, in order to enable easier positioning of wheel face laminations and assembly of balsa wood spacers and spring clamps. For horizontal assembly process torsion box shown in figure 37 was built and a test assembly of 750 kW machine's wheel face was done on top of it.



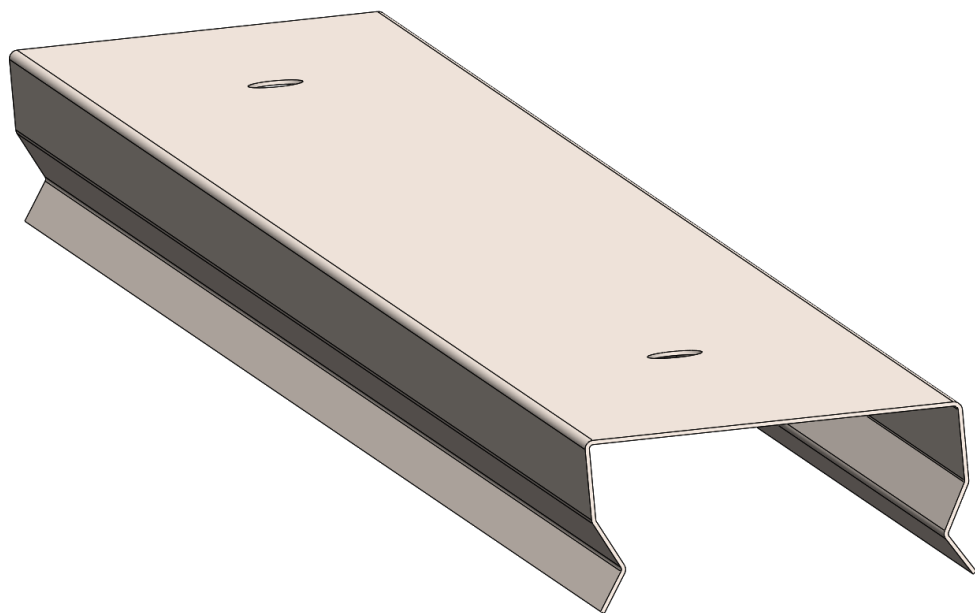
**Figure 37.** Assembled wheel face on top of torsion box.

As a result of test assembly of one wheel face a tool for more effective assembly of spring clamps was proposed to be made. During the same assembly spacer tools were tested. Using the wheel face assembly spacers between torsion box and wheel face stack prevents wheel

face laminations from sagging. The final design of spacer tool proved to be functional and easy to manufacture as 50% of the parts could be manufactured from the same metal sheet using the same cutting method.

Spring clamps manufactured from 0.5 mm thick stainless spring steel were tested on prototype wheel face. The initial thicknesses for spring clamps were 0.5 mm and 0.8 mm. The FE analyses of the clamp with both thicknesses showed that local peak stresses of 0.8 mm thick clamp exceeded material's tensile strength even with halved forces. The local peak stresses of 0.5 mm thick clamps also exceeded tensile strength of the material, by 16%. The practical test of clamps proved that 0.5 mm thick spring clamp can be installed to the wheel face without any damage. The practical test also proved that results from Femap analyses do not correspond with actual part. The reason for incorrect results of Femap analyses may be found in constrains of the analyzed part. The results of Femap analyses and analytical calculation may be evaluated better if clamping force would be measured for example by using pressure sensors.

After the practical test 0.5 mm thick clamps were considered easy to assemble and their clamping force was satisfactory. The spring clamps were further developed and slots on the sides were removed as there was no need for clevis pins in proof of concept prototype. The developed clamp is shown in figure 38.



**Figure 38.** Updated design of spring clamp.

Removal of clevis pin slots from the sides of clamp may improve the stiffness of the clamp and increase its clamping force.

Selection of the coating for electrical steel laminations was done by comparing properties of different SURALAC coatings and testing of three sample pieces with different coatings. As electrical steel laminations are not welded in LWLC machine, friction between individual sheets was considered as an important factor. For testing the friction sample pieces were ordered with three different coatings. The test was done by sliding test pieces against each other to determine which coating had the highest friction. As a result SURALAC 7000 was chosen as suitable coating for electrical steel laminations in LWLC machine.

For binding electrical steel laminations of rotor and stator segments fiberglass bolts were proposed. In order to determine binding force and tension in the rod a test was done to a stud bolt made of fiberglass. The bolt was tested in non-lubricated form and lubricated form. Tightening of the bolt was done gradually starting from low torque values. The tightening test showed that when tightened to the recommended torque value in lubricated form the fiberglass stud bolt can provide 48% higher binding force compared to non-lubricated form. The tension inside the rod was also 48% higher in lubricated form compared to non-lubricated form. Estimated binding force value was 2400 N and tension value 42 MPa. The test bolt did not suffer major damage and withstood recommended installation torque. On the basis of the test fiberglass binding rods were considered suitable for LWLC machine. Proposed fiberglass binding rod with square nuts is shown in figure 39.



**Figure 39.** Fiberglass binding rod with two square nuts.

The proposed fiberglass bolts are 340 mm long and they can be used in both rotor and stator segment assemblies.

Balsa wood spacers were used as filling material between wheel face laminations. As a light material with good energy dissipation and high axial strength balsa was suitable for LWLC machine's lightweight structure. Initial balsa parts were designed to be 19 mm thick. Test pieces for rotor and stator rim balsa parts were machined by using CNC milling machine and the right thickness was achieved by using surface grinder. CNC machining was considered as suitable option for manufacturing balsa parts for LWLC machine. Balsa parts for proof of concept machine were re-designed to be 16 mm thick in rotor and 22 mm in stator as a response to static structural analysis made by a member of the project.

Further development of parts for LWLC machine can be made after first prototype machine will be built. Possible further include clamp assembly tool, base structure for torsion box and a stand for LWLC machine. Clamp assembly tool was proposed in order to assist the assembly process of spring clamps. The tool should be operable by hand and it may use the round slot between two spokes as support point. The base structure under the torsion box may be re-designed as the initial base was built using steel pipes. New base structure may also use pipes but it should be more stable as initial structure is vulnerable to horizontal displacements. The functionality of clamps, fiberglass binding rods, balsa spacers and electrical steel laminations can be better evaluated after first tests of proof of concept LWLC machine.

## REFERENCES

Boothroyd, G., Dewhurst, P. & Knight, W. 2002. Product Design for Manufacture and Assembly. Second edition. Boca Raton: CRC Press. 698 p.

Cogent. 2016. Non-oriented electrical steel [web document]. Surahammar: 2016 [Referred 12.2.2017]. Available in PDF-file: <https://cogent-power.com/cms-data/downloads/Cogent%20NO%20brochure%202016.pdf>

Cook, R., D. 1995. Finite Element Modeling for Stress Analysis. Madison: John Wiley & Sons, Inc. 320 p.

ESAB. 2013. Education. [ESAB webpage]. Updated July 29, 2013. [Referred: 15.2.2017]. Available: <http://www.esabna.com/us/en/education/blog/how-does-laser-cutting-work.cfm>

Fiberglass Studs & Nuts. 2017. [www- data sheet]. (Publishing place unknown): Strongwell, 2017. [Referred 27.1.2017]. Available: <https://www.strongwell.com/wp-content/uploads/2013/04/FIBREBOLT-Flyer.pdf>

Heikkilä, T. 2002. Permanent Magnet Synchronous Motor for Industrial Inverter Applications – Analysis and Design [web document]. Stockholm: October 2002 [Referred 8.5.2017]. Doctoral degree thesis. Lappeenranta University of Technology. 107 p. + appendixes 3 p. Available in PDF-file: <http://www.doria.fi/bitstream/handle/10024/31173/TMP.objres.359.pdf?sequence=1>

Lampola, P. 2000. Directly Driven, Low-Speed Permanent-Magnet Generators for Wind Power Applications [web document]. Espoo: March 2000 [Referred 8.5.2017]. Doctoral degree thesis. Helsinki University of Technology. 62 p. Available in PDF-file: <http://lib.tkk.fi/Diss/2000/isbn9512256924/isbn9512256924.pdf>

Lindenmo, M., Coombs, A. & Snell, D. 2000. Advantages, properties and types of coatings on non-oriented electrical steels. *Journal of Magnetism and Magnetic Materials*, 215-216. Pp. 79-82

Matilainen, J., Parviainen, M., Havas, T., Hiitelmä, E. & Hultin, S. 2011. *Ohutlevytuotteiden suunnittelijan käsikirja*. Tampere: Tammerprint Oy. 387 p.

Nutakor, C., Semken, R., S., Sopanen, J. & Mikkola, A. 2015. Vibration Analysis of a Novel Stator Wheel Structure for a Direct-Drive PM Generator. The 14<sup>th</sup> IFToMM World Congress. Taipei, Taiwan. 25-30.10.2015.

Outokumpu. 2015. Properties by product. [Outokumpu webpage]. Updated 2015. [Referred 29.3.2017]. Available: <http://steelfinder.outokumpu.com/Properties/GradeDetail.aspx?OKGrade=4301&Category=Core>

Pahl, G., Beitz, W., Feldhusen, J. & Grote, K-H. 2007. *Engineering Design: A Systematic Approach*. Translated from German and edited by Ken Wallace and Luciënne Blessing. Third edition. London: Springer. 617 p.

Petrovič, D., S. 2010. Non-oriented Electrical Steel Sheets. *Materiali in tehnologije / Materials and technology*, 44: 6. Pp. 317-325.

Prima Power. 2013. Servo-electric bending technology by Prima Power [web document]. Publishing place unknown: February 2013 [Referred 14.2.2017]. Available in PDF-file: [http://www.primaindustrie.com/uploads/editorialtext/docs/300GB\\_Feb2013\\_\\_eP-1030.pdf](http://www.primaindustrie.com/uploads/editorialtext/docs/300GB_Feb2013__eP-1030.pdf)

Prima Power. 2017. The Laser 3D line [web document]. Publishing place unknown: January 2017 [Referred 16.2.2017]. Available in PDF-file: <http://www.primapower.com/wp-content/uploads/2017/02/Prima-power-3D-laser.pdf>

Sandvik. 2003. Stainless steels for spring and other demanding applications [web document]. Sandviken: January 2003 [Referred 27.3.2017]. Available in PDF-file: [http://smt.sandvik.com/globalassets/global/downloads/products\\_downloads/strip-steel-and-strip-based-products/stainless-steels-for-springs-and-other-demanding-applications-3411-eng.sept.2002.pdf](http://smt.sandvik.com/globalassets/global/downloads/products_downloads/strip-steel-and-strip-based-products/stainless-steels-for-springs-and-other-demanding-applications-3411-eng.sept.2002.pdf)

Semken, S., Polikarpova, M., Røyttä, P., Alexandrova, J., Pyrhönen, J., Nerg, J., Mikkola, A. & Backman, J. 2012. Direct-drive permanent magnet generators for high-power wind turbines: benefits and limiting factors. *IET Renewable Power Generation*, 6: 1. Pp. 1-8.

Semken, R., S. 2015. *Lightweight, Liquid-Cooled, Direct-Drive Generator for High-Power Wind Turbines: Motivation, Concept, and Performance*. Lappeenranta: Yliopistopaino. 135 p.

SFS-EN 10088-2. 2014. *Ruostumattomat teräkset. Osa 2: Yleiseen käyttöön tarkoitetut korroosionkestävät levyt ja nauhat. Tekniset toimitusehdot*. Helsinki: Suomen Standardisoimisliitto SFS. 106 p. Confermed and published in English.

Silva, A., D. & Kyriakides, S. 2007. Compressive response and failure of balsa wood. *International Journal of Solids and Structures*, 44: 25-26. Pp. 8685-8717.

Tap Chart-UNC/UNF Threads. 2003. [www- data sheet]. (Publishing place unknown): Carbide Depot, 2003. [Referred 27.1.2017]. Available: <http://www.carbidedepot.com/formulas-tap-standard.htm>

Valtanen, E. 2010. *Tekniikan taulukkikirja*. 18<sup>th</sup> edition. Jyväskylä: Genesis – kirjat Oy. 1176 p.

Vural, M. & Ravichandran, G. 2003. Dynamic response and energy dissipation characteristics of balsa wood: experiment and analysis. *International Journal of Solids and Structures*, 40: 9. Pp. 2147-2170.

Wallenberger, F., T. & Bingham, P., A. *Fiberglass and Glass Technology: Energy – Friendly Compositions and Applications*. New York: Springer. 474 p.

Clamping force calculations. In this appendix calculation for longer part of the clamp is presented.

### Clamping force calculation for wheel face lamination clamps

Clamp assumed as a beam with fixed end and free end.

Force position:

$a := 15\text{mm}$  From fixed end

$b := 5\text{mm}$  From free end

Profile dimensions:

$b_1 := 254.631\text{mm}$  Width

$h := 0.50\text{mm}$  Height

$l := 20\text{mm}$  Beam length

$$I := \frac{b_1 \cdot h^3}{12} = 2.652 \times 10^{-12} \text{ m}^4 \quad \text{Moment of inertia}$$

Material values:

$E := 200000\text{MPa}$  Elastic modulus

$f := 2\text{mm}$  Required translation

Force:

$$F := \frac{6 \cdot E \cdot I \cdot f}{(3 \cdot l \cdot a^2 - a^3)} = 628.719 \text{ N} \quad \text{From equation: } f = (Fa^3/6EI) \cdot ((3l/a)-1)$$

Moment in fixed end:

$$M_{\text{fixed}} := F \cdot a = 9.431 \cdot \text{N} \cdot \text{m}$$

Clamping force calculations. In this appendix calculation for shorter part of the clamp is presented.

### Clamping force calculation for wheel face lamination clamps

Clamp assumed as a beam with fixed end and free end.

Force position:

$a := 15\text{mm}$  From fixed end

$b := 5\text{mm}$  From free end

Profile dimensions:

$b_1 := 172.631\text{mm}$  Width

$h := 0.50\text{mm}$  Height

$l := 20\text{mm}$  Beam length

$$I := \frac{b_1 \cdot h^3}{12} = 1.798 \times 10^{-12} \text{m}^4 \quad \text{Moment of inertia}$$

Material values:

$E := 200000\text{MPa}$  Elastic modulus

$f := 2\text{mm}$  Required translation

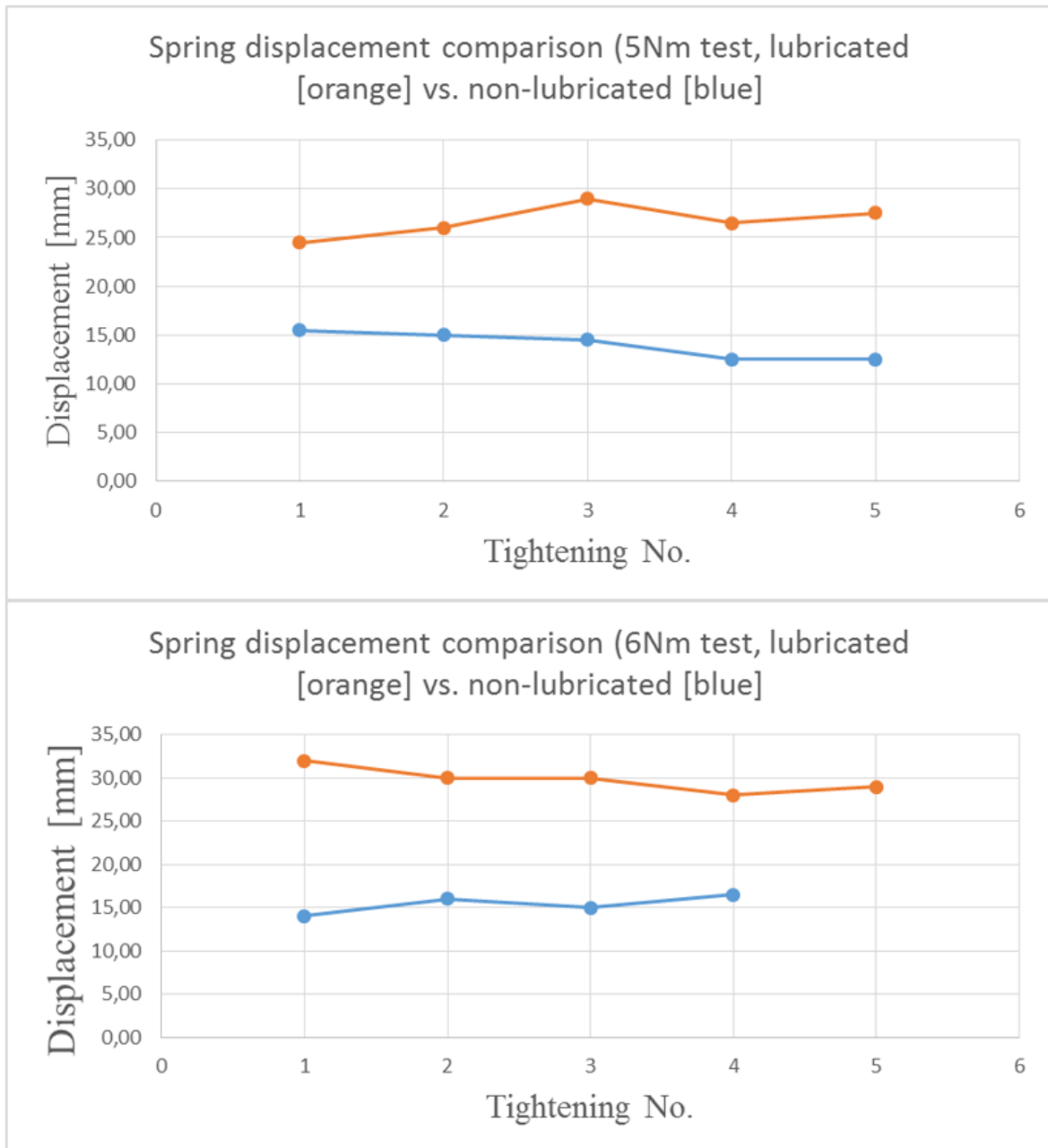
Force:

$$F := \frac{6 \cdot E \cdot I \cdot f}{(3 \cdot l \cdot a^2 - a^3)} = 426.249 \text{N} \quad \text{From equation: } f = (Fa^3/6EI) \cdot ((3l/a) - 1)$$

Moment in fixed end:

$$M_{\text{fixed}} := F \cdot a = 6.394 \cdot \text{N} \cdot \text{m}$$

Result charts of fiberglass vinyl ester stud bolt test. Displacements of 5 Nm and 6 Nm tests, non – lubricated and lubricated.



Result charts of fiberglass vinyl ester stud bolt test. Displacement and force comparison of non – lubricated and lubricated tests. Displacements presented are average displacements.

